2012-03

# High Impact Weather Associated with a Predecessor Rain Event Over Misawa Air Base

Svatek, Mike E.

Monterey, California. Naval Postgraduate School


# NAVAL POSTGRADUATE SCHOOL

**MONTEREY, CALIFORNIA**

# THESIS

**HIGH IMPACT WEATHER ASSOCIATED WITH A PREDECESSOR RAIN EVENT OVER MISAWA AIR BASE**

by

Mike E. Svatek

March 2012

| | |
|---|---|
| Thesis Advisor: | Patrick Harr |
| Second Reader: | Richard Moore |

**Approved for public release; distribution is unlimited**

THIS PAGE INTENTIONALLY LEFT BLANK

| REPORT DOCUMENTATION PAGE | | | Form Approved OMB No. 0704-0188 |
|---|---|---|---|
| Public reporting burden for this collection of information is estimated to average 1 hour per response, including the time for reviewing instruction, searching existing data sources, gathering and maintaining the data needed, and completing and reviewing the collection of information. Send comments regarding this burden estimate or any other aspect of this collection of information, including suggestions for reducing this burden, to Washington headquarters Services, Directorate for Information Operations and Reports, 1215 Jefferson Davis Highway, Suite 1204, Arlington, VA 22202-4302, and to the Office of Management and Budget, Paperwork Reduction Project (0704-0188) Washington DC 20503. | | | |
| **1. AGENCY USE ONLY** ***(Leave blank)*** | **2. REPORT DATE** March 2012 | **3. REPORT TYPE AND DATES COVERED** Master's Thesis | |
| **4. TITLE AND SUBTITLE** High Impact Weather Associated with a Predecessor Rain Event Over Misawa Air Base | | **5. FUNDING NUMBERS** | |
| **6. AUTHOR(S)** Mike E. Svatek | | | |
| **7. PERFORMING ORGANIZATION NAME(S) AND ADDRESS(ES)** Naval Postgraduate School Monterey, CA 93943-5000 | | **8. PERFORMING ORGANIZATION REPORT NUMBER** | |
| **9. SPONSORING /MONITORING AGENCY NAME(S) AND ADDRESS(ES)** N/A | | **10. SPONSORING/MONITORING AGENCY REPORT NUMBER** | |
| **11. SUPPLEMENTARY NOTES** The views expressed in this thesis are those of the author and do not reflect the official policy or position of the Department of Defense or the U.S. Government. IRB Protocol number _____N/A_____. | | | |
| **12a. DISTRIBUTION / AVAILABILITY STATEMENT** spproved for public release; distribution is unlimited | | **12b. DISTRIBUTION CODE** A | |

**13. ABSTRACT (maximum 200 words)**

Two significant rain events of greater than 100 mm 24 $h^{-1}$ occurred over Japan in direct association with tropical moisture transport from Typhoon (TY) Roke in September 2011. The first event occurred over Misawa Air Base, Japan during 17–19 September 2011. Based on analysis of satellite imagery and numerical simulations, the Misawa rain event is classified as a predecessor rain event (PRE). A PRE is defined as a region of heavy rainfall that occurs thousands of kilometers poleward of a tropical cyclone (TC). The second rain event occurred over Nagasaki on 18 September 2011 and does not meet the requirements for PRE classification. The Department of Defense (DoD) TC warning process focuses on TC induced sustained high winds and their proximity to landfall. This analysis shows the link between the Misawa PRE and Roke via the poleward transport of deep tropical moisture. Because excessive rainfall is considered a destructive force associated with TCs, it is the purpose of this thesis that the U.S. Navy's tropical cyclone conditions of readiness (TCCOR) procedures reflect PRE conditions in order to raise awareness within all meteorology communities amongst the DoD in efforts to minimize risks to DoD installations and personnel.

| **14. SUBJECT TERMS** Tropical Cyclone, Typhoon, Warning, TCCOR, Predecessor Rain Event, PRE, Precipitable Water, PW, Misawa, Japan, OPNAVINST | | | **15. NUMBER OF PAGES** 79 |
|---|---|---|---|
| | | | **16. PRICE CODE** |
| **17. SECURITY CLASSIFICATION OF REPORT** Unclassified | **18. SECURITY CLASSIFICATION OF THIS PAGE** Unclassified | **19. SECURITY CLASSIFICATION OF ABSTRACT** Unclassified | **20. LIMITATION OF ABSTRACT** UU |

NSN 7540-01-280-5500

Standard Form 298 (Rev. 2-89)
Prescribed by ANSI Std. 239-18

THIS PAGE INTENTIONALLY LEFT BLANK

**Approved for public release; distribution is unlimited**

# HIGH IMPACT WEATHER ASSOCIATED WITH A PREDECESSOR RAIN EVENT OVER MISAWA AIR BASE

Mike E. Svatek
Lieutenant Commander, United States Navy
B.S., Texas A&M University, 2001
M.E.M., Old Dominion University, 2007

Submitted in partial fulfillment of the requirements for the degree of

**MASTER OF SCIENCE IN METEOROLOGY AND OCEANOGRAPHY**

from the

**NAVAL POSTGRADUATE SCHOOL**
**March 2012**

Author: Mike E. Svatek

Approved by: Patrick Harr
Thesis Advisor

Richard Moore
Second Reader

Wendell A. Nuss
Chair, Department of Meteorology and Physical Oceanography

THIS PAGE INTENTIONALLY LEFT BLANK

# ABSTRACT

Two significant rain events of greater than 100 mm 24 $h^{-1}$ occurred over Japan in direct association with tropical moisture transport from Typhoon (TY) Roke in September 2011. The first event occurred over Misawa Air Base, Japan during 17–19 September 2011. Based on analysis of satellite imagery and numerical simulations, the Misawa rain event is classified as a predecessor rain event (PRE). A PRE is defined as a region of heavy rainfall that occurs thousands of kilometers poleward of a tropical cyclone (TC). The second rain event occurred over Nagasaki on 18 September 2011 and does not meet the requirements for PRE classification. The Department of Defense (DoD) TC warning process focuses on TC induced sustained high winds and their proximity to landfall. This analysis shows the link between the Misawa PRE and Roke via the poleward transport of deep tropical moisture. Because excessive rainfall is considered a destructive force associated with TCs, it is the purpose of this thesis that the U.S. Navy's tropical cyclone conditions of readiness (TCCOR) procedures reflect PRE conditions in order to raise awareness within all meteorology communities amongst the DoD in efforts to minimize risks to DoD installations and personnel.

THIS PAGE INTENTIONALLY LEFT BLANK

# TABLE OF CONTENTS


I. INTRODUCTION....1
A. MOTIVATION....1
1. Tropical Storms and Predecessor Rain Events....1
2. Predecessor Rain Events and the United States Navy....2
B. OBJECTIVE....3

II. BACKGROUND....5
A. PREDECESSOR RAIN EVENT (PRE) CRITERIA....5
B. TROPICAL CYCLONE CONDITIONS OF READINESS (TCCOR)....8
1. Defining Conditions of Readiness....8
2. Setting Tropical Cyclone Conditions of Readiness....10
*a. Fleet Activities Sasebo....11*
*b. Misawa Air Base....14*

III. METHODOLOGY....17
A. DATA....17
1. Satellite Imagery....17
2. Rainfall Data....18
3. TCCOR Data....20
4. Tropical Cyclone Roke Track Data....21
B. MODEL SIMULATION....24
1. Global Forecasting System (GFS) Model....24
2. Weather Research and Forecasting (WRF) Model....25
3. Model Characteristics....26

IV. ANALYSIS AND RESULTS....31
A. MISAWA PREDECESSOR RAIN EVENT....31
1. Rainfall Analysis....31
2. PRE Characteristics....34
B. MISAWA STORM EVENT....45
C. NAGASAKI SIGNIFICANT RAIN EVENT....47

V. CONCLUSION AND RECOMMENDATION....51
A. MISAWA AIR BASE PRE IMPACTS....51
B. NAGASAKI SIGNIFICANT RAIN EVENT IMPACTS....53
C. OPNAVINST 3140.24F RECOMMENDATION....53

LIST OF REFERENCES....55

INITIAL DISTRIBUTION LIST....57

THIS PAGE INTENTIONALLY LEFT BLANK

# LIST OF FIGURES


Figure 1. Overview schematics for the meteorological features associated with (a) PRE #1, (b) PRE #2, and (c) PRE #3 showing the location and intensity of PREs, 250 hPa jet ("J"; gray shading and thin dashed contours), 700 hPa trough axis (thick dashed black line) and height contours (solid black contours), lower-tropospheric jet [large red arrow in panel (c)], tropospheric moisture (light and dark blue shading representing precipitable water values >30 and >50 mm, respectively), tropical features (Ike: TC symbol, Lowell: TC and TD symbols, Bay of Campeche disturbance: "L"), surface frontal features, lower-tropospheric wind pattern near the frontal boundary and PRE in the warm (red-arrowed lines) and cool (magenta-arrowed lines) air, and surface cyclone and anticyclone locations given by the red "L" and blue "H" symbols, respectively (From Bosart et al. 2011) ..... 5

Figure 2. (a) Circulations injet-entrance and exit regions, (b) Jet-entrance region dynamics (After Moore 2004) ..... 7

Figure 3. Graphical depiction the Nagasaki Prefecture Region around Sasebo (After http://www.weather-forecast.com/locations/Sasebo) ..... 12

Figure 4. Graphical depiction Aomori Prefecture containing Misawa and Aomori (After http://www.weather-forecast.com/locations/Misawa) ..... 15

Figure 5. (a) Color enhanced METSAT-2 full disk infrared (IR) and (b) color enhanced METSAT-2 full disk water vapor for 0531 UTC 18 September 2011 over the Eastern Hemisphere (From http://www.ncdc.noaa.gov/) ..... 17

Figure 6. (a) METSAT-2 color enhanced IR imagery and (b) color enhanced water vapor imagery at 0932 UTC 17 September 2011 (from NRLMRY) ..... 18

Figure 7. (a) Blended 3-h rain accumulations and (b) blended 6-h rain accumulations at 0900 UTC 17 September 2011 (From NRLMRY) ..... 18

Figure 8. Aomori rainfall histogram with 12-h bin size for 0000 UTC 13 September 2011 through 1200 UTC 24 September 2011 ..... 20

Figure 9. TY Roke TCCOR timeline showing DoD TCCOR posture with respect to TY Roke landfall (red dashed line) for military installations within USFJ ..... 21

Figure 10. The TCFA graphic for 1800 UTC 10 September 2011 (From JTWC) ..... 22

Figure 11. Typhoon Roke best track analysis (After http://en.wikipedia.org/wiki/File:Roke_2011_track.png) ..... 23

Figure 12. Analyzed GFS fields of precipitable water (shaded in mm), sea-level pressure (solid black line in hPA), and 1000-500 hPA thickness (red dashed line in dam) for 1200 UTC 18 September 2011 (From http://www.atmos.albany.edu/student/heathera/slp_thick/wpac/7_to_22_sep.html) ..... 24

Figure 13. Analyzed GFS field of 700 hPa height contour (dam), Q-vector (scale at lower left in units $10^{-7}$ Pa $m^{-1}$ $s^{-1}$), and quasi-geostrophic forcing of vertical motion (shaded in units of $10^{-12}$ Pa $m^{-2}$ $s^{-1}$) for 1200 UTC 18 September 2011 (From http://www.atmos.albany.edu/student/heathera/qvect/wpac/7_to_22_sep.html) ..... 25

Figure 14. (a) WRF 27-km forecast and (b) WRF 9-km forecast of precipitable water (shaded in mm), sea-level pressure (solid black line in hPA), and 1000–500 hPA thickness

(red dashed line in dam) for 1200 UTC 17 September 2011 (After http://www.met.nps.edu/~hmarcham/roke/) ....26
Figure 15. TC Roke track comparison of JMA best track (black line), GFS (0.5 deg.) analyses (red line), WRF (27-km) forecast track 1 from 1200 UTC 16 September 2011 through 1200 UTC 22 September 2011 (blue line), and WRF (27-km) forecast track 2 from 1200 UTC 19 September 2011 through 1200 UTC 24 September 2011 (green line) where diamonds denote 0000 UTC times and dots denote 0600, 1200, and 1800 UTC times (After http://www.met.nps.edu/~hmarcham/roke/) ....27
Figure 16. TC Roke MSLP Comparison of JMA best track (black line), GFS (0.5 deg.) analyses (red line), WRF (27-km) forecast track 1 from 1200 UTC 16 September 2011 through 1200 UTC 22 September 2011 (blue line), and WRF (27-km) forecast track 2 from 1200 UTC 19 September 2011 through 1200 UTC 24 September 2011 (green line), shaded rain events PRE(STORM) on left(right) with max 24 h rain period shaded in red (After http://www.met.nps.edu/~hmarcham/roke/) ....28
Figure 17. Misawa rainfall histogram with 12-h bin size for 0000 UTC 13 September 2011 through 1200 UTC 24 September 2011 collected from NCDC ....31
Figure 18. Radar derived hourly rain rates (mm $h^{-1}$) for (a) 0000 UTC 17 September 2011, (b) 1200 UTC 17 September 2011, (c) 0000 UTC 18 September 2011, (d) 1200 18 September 2011 (After JMA) ....32
Figure 19. WRF-1 (9-km) forecast of accumulated rainfall (mm) for 0900 UTC 17 September 2011 through 0900 UTC 18 September 2011(After http://www.met.nps.edu/~hmarcham/roke/) ....33
Figure 20. Analyzed GFS fields of 1000–500 hPA thickness (dashed lines in dam), precipitable water (shaded in mm), sea-level pressure (solid black line in hPA), 250 hPa wind speed (m $s^{-1}$, shaded according to color bar) for (a) 1200 UTC 14 September 2011, (c) 1200 UTC 15 September 2011 (From http://www.atmos.albany.edu/student/heathera/slp_thick/wpac/7_to_22_sep.html), color enhanced METSAT-2 full disk IR for (b) 1131 UTC 14 September 2011, (d) 1131 UTC 15 September 2011 (After http://www.ncdc.noaa.gov/) ....34
Figure 21. Analyzed GFS fields of 1000–500 hPA thickness (dashed lines in dam), precipitable water (shaded in mm), sea-level pressure (solid black line in hPA), 250 hPa wind speed (m $s^{-1}$, shaded according to color bar) for (a) 1200 UTC 16 September 2011, (c) 1200 UTC 17 September 2011 (From http://www.atmos.albany.edu/student/heathera/slp_thick/wpac/7_to_22_sep.html), color enhanced METSAT-2 full disk IR for (b) 1131 UTC 16 September 2011, (d) 1131 UTC 17 September 2011 (After http://www.ncdc.noaa.gov/) ....35
Figure 22. WRF-1 (9-km) forecast of 200 hPa wind (barbs, kt), 800–400 hPa layer-averaged ascent (red contours every 2 m $s^{-1}$, starting at 0.5 m $s^{-1}$), SLP (black contours every 4 hPa), total precipitable water (shaded in mm according to gray scale) for (a) 0000 UTC 17 September 2011, (b) 1200 UTC 17 September 2011, (c) 0000 UTC 18 September 2011, (d) 1200 UTC 18 September 2011 (After http://www.met.nps.edu/~hmarcham/roke/) ....36
Figure 23. WRF-1 (27-km) forecast of 250 hPa wind speed (m $s^{-1}$, shaded according to color bar), 1000–500 hPa thickness (dashed contours every 6 dam), SLP (solid contours every 4 hPa), total precipitable water (mm, shaded according to gray scale) for (a)

1200 UTC 17 September 2011, (b) 0000 UTC 18 September 2011. (c) 1200 UTC 18 September 2011, (d) 0000 UTC 19 September 2011 (After http://www.met.nps.edu/~hmarcham/roke/) ....37
Figure 24. (a) WRF-1 (27-km) forecast of 700 hPa geopotential height (solid blue, dam), temperature (dashed red, °C), Q vector (arrows, plotted for values greater than 5 x $10^{-7}$ Pa $m^{-1}$ $s^{-1}$ only), and Term A of the Q-vector form of the QG Omega equation (shaded $10^{-12}$ Pa $m^{-2}$ $s^{-1}$) for 1200 UTC 17 September 2011, and (b) WRF-1 (27-km) jet-entrance cross sections of PV (shaded, PVU), potential temperature (gray contours, every 5 K), ageostrophic wind (barbs, kt), frontogenesis (black contours, every 1 °C 100 $km^{-1}$ 3 $h^{-1}$, mixing ratio (blue contours, every 5 g $kg^{-1}$), ascent (green contours, every 1 m $s^{-1}$) for 1200 UTC 17 September 2011 (After http://www.met.nps.edu/~hmarcham/roke/) ....38
Figure 25. WRF-1 (27-km) jet-entrance cross section forecast of PV (shaded, PVU), potential temperature (gray contours, every 5 K), full wind (barbs, kt), jet core wind speed (black contours, every 10 m $s^{-1}$, starting at 40 m $s^{-1}$, mixing ratio (blue contours, every 5 g $kg^{-1}$), ascent (green contours, every 1 m $s^{-1}$) for (a) 1200 UTC 17 September 2011, (b) 0000 UTC 18 September 2011, (c) 1200 UTC 18 September 2011, (d) 0000 UTC 19 September 2011 (After http://www.met.nps. edu/~hmarcham/roke/) ....39
Figure 26. (a) WRF-1 (27-km) forecast of 700 hPa geopotential height (solid blue, dam), temperature (dashed red, °C), Q vector (arrows, plotted for values greater than 5 x $10^{-7}$ Pa $m^{-1}$ $s^{-1}$ only), and Term A of the Q-vector form of the QG Omega equation (shaded $10^{-12}$ Pa $m^{-2}$ $s^{-1}$) for 0000 UTC 18 September 2011, and (b) WRF-1 (27-km) jet-entrance cross sections of PV (shaded, PVU), potential temperature (gray contours, every 5 K), ageostrophic wind (barbs, kt), frontogenesis (black contours, every 1 °C 100 $km^{-1}$ 3 $h^{-1}$, mixing ratio (blue contours, every 5 g $kg^{-1}$), ascent (green contours, every 1 m $s^{-1}$) for 0000 UTC 18 September 2011 (After http://www.met.nps.edu/~hmarcham/roke/) ....41
Figure 27. (a) WRF-1 (27-km) forecast of 700 hPa geopotential height (solid blue, dam), temperature (dashed red, °C), Q vector (arrows, plotted for values greater than 5 x $10^{-7}$ Pa $m^{-1}$ $s^{-1}$ only), and Term A of the Q-vector form of the QG Omega equation (shaded $10^{-12}$ Pa $m^{-2}$ $s^{-1}$) for 1200 UTC 18 September 2011, and (b) WRF-1 (27-km) jet-entrance cross sections of PV (shaded, PVU), potential temperature (gray contours, every 5 K), ageostrophic wind (barbs, kt), frontogenesis (black contours, every 1 °C 100 $km^{-1}$ 3 $h^{-1}$, mixing ratio (blue contours, every 5 g $kg^{-1}$), ascent (green contours, every 1 m $s^{-1}$) for 1200 UTC 18 September 2011 (After http://www.met.nps.edu/~hmarcham/roke/) ....42
Figure 28. (a) WRF-1 (27-km) forecast of 700 hPa geopotential height (solid blue, dam), temperature (dashed red, °C), Q vector (arrows, plotted for values greater than 5 x $10^{-7}$ Pa $m^{-1}$ $s^{-1}$ only), and Term A of the Q-vector form of the QG Omega equation (shaded $10^{-12}$ Pa $m^{-2}$ $s^{-1}$) for 0000 UTC 19 September 2011, and (b) WRF-1 (27-km) jet-entrance cross sections of PV (shaded, PVU), potential temperature (gray contours, every 5 K), ageostrophic wind (barbs, kt), frontogenesis (black contours, every 1 °C 100 $km^{-1}$ 3 $h^{-1}$, mixing ratio (blue contours, every 5 g $kg^{-1}$), ascent

(green contours, every 1 m $s^{-1}$) for 0000 UTC 19 September 2011 (After http://www.met.nps.edu/~hmarcham/roke/) .....44
Figure 29. (a) WRF-2 (27-km) forecast of 700 hPa geopotential height (solid blue, dam), temperature (dashed red, °C), Q vector (arrows, plotted for values greater than 5 x $10^{-7}$ Pa $m^{-1}$ $s^{-1}$ only), and Term A of the Q-vector form of the QG Omega equation (shaded according to the colorbar, $10^{-12}$ Pa $m^{-2}$ $s^{-1}$) for 1200 UTC 21 September 2011, and (b) WRF-2 (27-km) jet-entrance region cross section of PV (shaded, PVU), potential temperature (gray contours, every 5 K), full wind (barbs, kt), wind speed (black contours, every 10 m $s^{-1}$, starting at 40 m $s^{-1}$, mixing ratio (blue contours, every 5 g $kg^{-1}$), ascent (green contours, every 1 m $s^{-1}$) for 1200 UTC 21 September 2011 (After http://www.met.nps.edu/~hmarcham/roke/) .....45
Figure 30. (a) WRF-2 (27-km) forecast of 700 hPa geopotential height (solid blue, dam), temperature (dashed red, °C), Q vector (arrows, plotted for values greater than 5 x $10^{-7}$ Pa $m^{-1}$ $s^{-1}$ only), and Term A of the Q-vector form of the QG Omega equation (shaded according to the colorbar, $10^{-12}$ Pa $m^{-2}$ $s^{-1}$) for 1800 UTC 21 September 2011, and WRF-2 (27-km) along track cross-section of PV (shaded, PVU), potential temperature (gray contours, every 5 K), ageostrophic wind (barbs, kt), frontogenesis (black contours, every 1 °C 100 $km^{-1}$ 3 $h^{-1}$, mixing ratio (blue contours, every 5 g $kg^{-1}$), ascent (green contours, every 1 m $s^{-1}$) for (b) 0600 UTC 21 September 2011, (c) 1200 UTC 21 September 2011, and (d) 1800 UTC 21 September 2011. (After http://www.met.nps.edu/~hmarcham/roke/) .....46
Figure 31. Nagasaki rainfall histogram with 12 h bin size for 0000 UTC 13 September 2011 through 1200 UTC 24 September 2011 collected from NCDC.....47
Figure 32. (a) WRF-1 (27-km) forecast of 700 hPa geopotential height (solid blue, dam), temperature (dashed red, °C), Q vector (arrows, plotted for values greater than 5 x $10^{-7}$ Pa $m^{-1}$ $s^{-1}$ only), and Term A of the Q-vector form of the QG Omega equation (shaded according to the colorbar, $10^{-12}$ Pa $m^{-2}$ $s^{-1}$) for 1200 UTC 18 September 2011, and (b) WRF-1 (27-km) forecast of 250 hPa wind speed (m $s^{-1}$, shaded according to color bar), 1000–500 hPa thickness (dashed contours every 6 dam), SLP (solid contours every 4 hPa), total precipitable water (mm, shaded according to gray scale) for 1200 UTC 18 September 2011 (After http://www.met.nps.edu/~/hmarcham/roke/) .....48
Figure 33. (a) Radar derived hourly rain rates (mm $h^{-1}$) for 1200 UTC 18 September 2011, and WRF-1 (9-km) forecast of 1 h accumulated rainfall (mm) for (b) 0900 UTC 18 September 2011, (c) 1000 UTC 18 September 2011, (d) 1100 UTC 18 September 2011 (After http://www.met.nps.edu/~hmarcham/roke/) .....49
Figure 34. TS Roke warning #22 for 1800 UTC on 16 September 2011, (From JTWC).....52

THIS PAGE INTENTIONALLY LEFT BLANK

# LIST OF TABLES

Table 1. U.S. Navy Conditions of Readiness (From OPNAVINST 3140.2F) .....9
Table 2. U.S. Air Force OPREP-3 reporting requirements (From AF 10-206).....10
Table 3. NOAC, Yokosuka TCCOR thresholds (From Commander NOAC, Yokosuka SOP) ...13
Table 4. Fleet Activities Sasebo Thunderstorm Warning Criteria (From Commander, Fleet Activities Sasebo 2010) .....14
Table 5. Max 24-h vs. Total accumulated rainfall for PRE and TC Roke.....19

THIS PAGE INTENTIONALLY LEFT BLANK

# LIST OF ACRONYMS AND ABBREVIATIONS

**AB:** Air Base

**AT:** Along TC Track

**COR:** Condition of Readiness

**CPA:** Closest Point of Approach

**DOAF:** Department of the Air Force

**DoD:** Department of Defense

**DON:** Department of the Navy

**DTG:** Date Time Group

**ET:** Extra-Tropical Transition

**FAS:** Fleet Activities Sasebo

**GFS:** Global Forecasting System (model)

**JMA:** Japan Meteorology Agency

**JTWC:** Joint Typhoon Warning Center

**LOT:** Left of TC Track

**METSAT:** Meteorological Satellite

**NCDC:** National Climatic Data Center

**NHC:** National Hurricane Center

**NMOC:** Navy Meteorology and Oceanography Command

**NOAA:** National Oceanographic and Atmospheric Administration

**NOAC:** Naval Oceanography Antisubmarine Warfare Center

**NRLMRY:** Naval Research Laboratory Monterey

**OOTN:** Oceanographer of the Navy

**PBL:** Planetary Boundary Layer

**PRE:** Predecessor Rain Event

**PW:** Precipitable Water

**PV:** Potential Vorticity

**QG:** Quasi-Geostrophic

**ROT:** Right of TC Track

**SLP:** Sea Level Pressure

**TC:** Tropical Cyclone

**TS:** Tropical Storm

**TCCOR:** Tropical Cyclone Condition of Readiness

**TUTT:** Tropical Upper Troposphere Trough

**USFK:** United States Forces Korea

**USFJ:** United States Forces Japan

**WPAC:** Western Pacific

**WRF:** Weather Research and Forecasting (model)

**WRF-1:** First WRF Forecast Simulation (1200 UTC 16–22 September 2011)

**WRF-2:** Second WRF Forecast Simulation (1200 UTC 19–24 September 2011)

**WSM:** WRF Single-Moment

THIS PAGE INTENTIONALLY LEFT BLANK

# ACKNOWLEDGMENTS

I would like to thank several people for their contributions throughout this thesis experience. First of all, I would like to thank my thesis advisor, Professor Patrick A. Harr. His knowledge and command of the subject matter in the fields of meteorology and tropical cyclone activity helped guide my motivation behind this thesis into something productive for the DoD which has the potential to save lives. Furthermore, completion of this thesis would not have been possible without the assistance of Dr. Heather H. Archambault, whose assistance in numerical model simulation and data delivery, expertise in the field of predecessor rain event dynamics, and unwavering patience and dedication to the project make her an invaluable asset to the field of meteorology and the Naval Postgraduate School in Monterey, CA. Other notable contributions to the completion of this thesis came from Ms. Naoko Kitabatake of MRI-JMA, Mr. Kim Richardson of NRL-MRY, Mr. Robert Creasey of NPS, and Mr. David Ramsaur of FNMOC. I would like to send a final thanks to the Airmen, Sailors, and Officers of the Joint Typhoon Warning Center Pearl Harbor, the Naval Oceanography Antisubmarine Warfare Center (NOAC) in Yokosuka, and the 35th Operations Support Squadron at Misawa Air Base who helped contribute to this thesis and who continue to maintain a vigilant watch on the ocean above and the ocean below us in support of our nation.

THIS PAGE INTENTIONALLY LEFT BLANK

# I. INTRODUCTION

## A. MOTIVATION

### 1. Tropical Storms and Predecessor Rain Events

The formation, intensification and movement of tropical cyclones (TCs) are significant threats to the United States Navy. When a TC makes landfall, that perceived danger then becomes imminent danger to Department of Defense (DoD) decision makers and crisis planners. An often overlooked byproduct of the TC is the formation and transport of a tropical moisture plume that originates within the internal dynamics of the cyclone. The moisture may then be transported poleward thousands of kilometers away from the cyclone center. Often, these moisture plumes will interact with synoptic features such as frontal systems associated with migrating mid-latitude extratropical cyclones that supply dynamical support for enhanced rainfall. The term predecessor rain event (PRE) was used by Cote (2007) to describe these phenomena. Due to the propagation of continuous midlatitude shortwave disturbances in both the Northern and Southern Hemispheres, prediction of the timing and location of PRE events is often quite difficult.

Because of the noticeable high-impact weather associated with PREs, they have become the subject of recent research (Galarneau et al. 2010). In particular, PREs have been identified as being linked to TC activity that may occur thousands of kilometers away. Furthermore, a PRE may occur well in advance of the storm itself (Schumacher et al. 2010). The occurrence of a PRE may lead to significant forecast errors due to the geographic distance between the cause (tropical cyclones) and effect (excessive rainfall) of these phenomena, and to numerical model formulation deficiencies (Schumacher et al. 2010).

Cote (2007) analyzed 47 PREs associated with 21 TCs between 1998 and 2006 associated with recurving TCs within the western north Atlantic. His research indicated that 26 PREs occurred left of the TC track (LOT), 9 occurred right of the TC track (ROT) and 12 occurred along the final TC track (AT). All PREs identified in Cote's study

occur, on average, approximately 1000 km poleward and 36 hours ahead of the actual TC at the time of the event. Galarneau et al. (2010) identified 28 PREs that occurred over the eastern continental United States between 1995 and 2008. Their research indicated that 17 PREs occurred LOT, 4 occurred ROT, and 7 occurred AT. Their research, more focused on the mechanics of PRE development, identified that of the 28 PREs, 17 with associated with an anti-cyclonically curved 200 hPa jet structure, 8 were associated with a cyclonically curved 200 hPa jet structure, and 3 of PRE upper-level jet structures were unclassifiable.

## 2. Predecessor Rain Events and the United States Navy

From the perspective of U.S. Navy crisis planning, current readiness condition thresholds, specifically tropical cyclone conditions of readiness (TCCOR), are primarily based on forecast arrival times and wind speeds of active tropical cyclones. The impact of extreme rainfall rates is missing altogether from the TCCOR recommendation process (DON 2008).

Further concern is generated from the fact that TC emergency planning is generally done by the civilian population when the threat of the TC track (and its associated dangers) is forecast to affect a specific location at a specific time. Given that 21 PREs occurred LOT, it is reasonable to assume that once the track of a recurving TC was forecast to not make landfall along the eastern seaboard (thereby staying over the western North Atlantic), emergency planning for the region subsided. Tropical cyclones forecast to make landfall along the Gulf Coast may also cause emergency planning along the eastern seaboard to be relaxed although 9 PREs occurred ROT (Cote 2007). The same arguments can be made for western North Pacific TCs with respect to mainland Japan, China, and South Korea.

Because of the high concentration of DoD installations along the eastern seaboard within U.S. Forces Japan (USFJ) and within U.S. Forces Korea (USFK), it is necessary that DoD forecasters and emergency planners not only be aware of the likelihood of occurrence and most probable timing of PREs and their effects, but also to be given the training and tools to adequately forecast their development and probable areas of location.

## B. OBJECTIVE

In this thesis, a quantitative analysis of the large-scale factors related to TCs is conducted in relation to the mid-latitude environments that contribute to the occurrence of PRE formation. A primary objective is to raise the awareness of PRE impacts with the U.S. Navy Meteorology and Oceanography Command (METOC). Specifically, two rain events associated with moisture outflow from Typhoon (TY) Roke are analyzed. In these cases heavy rainfall developed over the Japanese archipelago and caused significant impacts on DoD installations in Misawa and surrounding areas of Sasebo, in the Nagasaki prefecture.

Current DoD regulations within USFJ require threat conditions to be established for TCs based on forecast high wind events only (USFJ 2010). As seen in this case study, two extreme rain events occurred first at Misawa Air Base (AB) and then around the surrounding areas at Fleet Activities Sasebo (FAS). Both events were in conjunction with moisture outflow from TY Roke and warranted preventative attention of crisis planners and warning authorities within the region. The first event, considered a traditional PRE, occurred at Misawa Air Base (AB) on 17–18 September 2011, when 121 mm of total rain fell ahead of TY Roke and 84 mm fell in 24 hours. During this event, TC Roke was approximately 1900 km south southeast and TCCOR ALL CLEAR was in effect for Misawa AB. Likewise, near Sasebo, over the Nagasaki prefecture, a significant rain even occurred on 18 September 2011, when 112 mm of total rain fell ahead of TC Roke and 110 mm of rain fell in 24 hours while Sasebo remained in TCCOR ALL CLEAR due to TY Roke's approximate location 900 km to the south southeast and the projected storm path to remain east and offshore of FAS.

Based on these findings, it is then necessary to determine whether the U.S. Navy TCCOR criteria for DoD installations should be amended to incorporate PRE phenomena such that the potential destructive impacts of excessive rainfall are minimized.

# II. BACKGROUND

## A. PREDECESSOR RAIN EVENT (PRE) CRITERIA

Nearly all investigations of PRE characteristics have been conducted based on the synoptic condition that exist over North America in association with a TC over the Gulf of Mexico or the western Atlantic Ocean (e.g. Bosart et al 2012). Based on these studies, several criteria have been identified to define the evolution of a PRE (Figure 1).

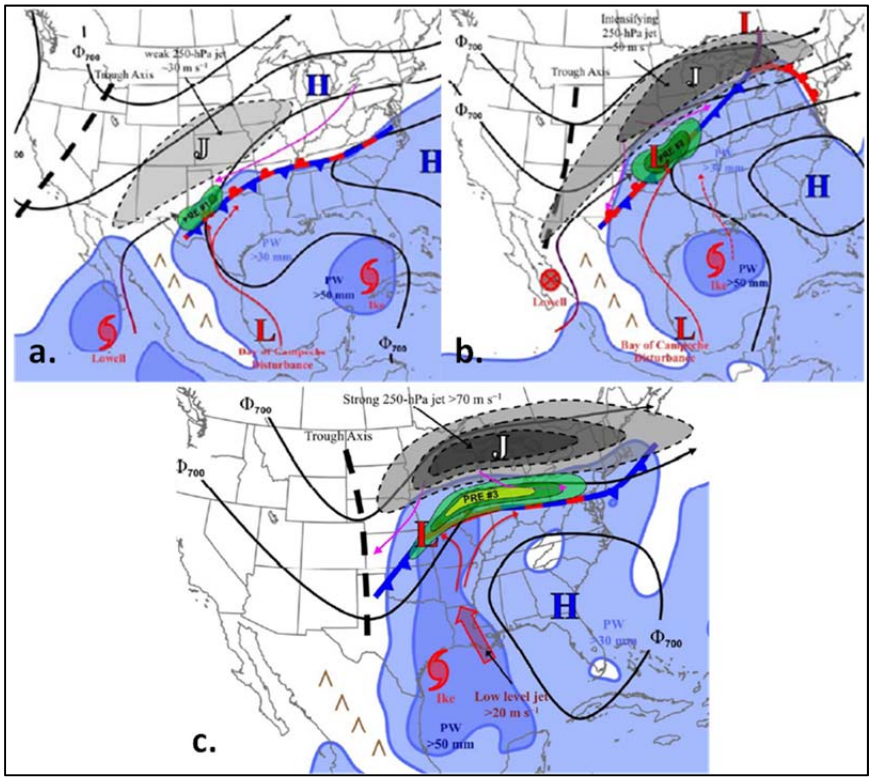


Figure 1. Overview schematics for the meteorological features associated with (a) PRE #1, (b) PRE #2, and (c) PRE #3 showing the location and intensity of PREs, 250 hPa jet ("J"; gray shading and thin dashed contours), 700 hPa trough axis (thick dashed black line) and height contours (solid black contours), lower-tropospheric jet [large red arrow in panel (c)], tropospheric moisture (light and dark blue shading representing precipitable water values >30 and >50 mm, respectively), tropical features (Ike: TC symbol, Lowell: TC and TD symbols, Bay of Campeche disturbance: "L"), surface frontal features, lower-tropospheric wind pattern near the frontal boundary and PRE in the warm (red-arrowed lines) and cool (magenta-arrowed lines) air, and surface cyclone and anticyclone locations given by the red "L" and blue "H" symbols, respectively (From Bosart et al. 2011)

First, the subsistence of a pre-existing, upper-level longwave trough (Figure 1a) that is favorable for the development midlevel frontogenesis is considered to be a favorable antecedent condition the development of a PRE (Cote 2007). At this time the TC is typically located far equator ward and the synoptic ridge may extend over the region poleward of the TC and equatorward of the baroclinic zone that is associated with the midlatitude trough. The location of the synoptic ridge at this time may prevent tropical moisture from extending poleward to interact directly with the baroclinic zone.

Second, an available moisture plume with precipitable water (PW) greater than 50 mm has been identified to be associated with PREs (Galarneau et al. 2010). The moisture plume develops as an embedded shortwave in the longwave pattern acts to force the subtropical high pressure ridge eastward. In response to the retreat of the subtropical ridge, the TC turns poleward and poleward moisture extends toward the midlatitude baroclinic zone (Figure 1b).

Often the PW of tropical origin is greater than 50 mm in magnitude. The advection of low-level moisture is usually due to southeasterly wind associated with an eastward migrating low-level equivalent potential temperature ($\theta_e$) ridge axis (Galarneau et al. 2010). Although recent studies have focused on the role of recurving TCs as being responsible for the poleward transport of high PW, poleward oriented moisture transport without the occurrence of TC recurvature may be responsible for PRE formation (Schumacher et al. 2010).

Third, many PREs are collocated with the upper-level jet-entrance region (Figure 1c) where the ageostrophic circulation acts to enhance vertical motion (Bosart et al. 2012). Dynamics of the quasi-geostrophic (QG) forced ageostrophic circulation associated with the jet-entrance region may be analyzed in terms of the Q-vector (Martin 2006).

The Q-vector form of the QG omega equation is $\left[\sigma\left(\nabla^2+\frac{f_o^2}{\sigma}\frac{\partial^2}{\partial p^2}\right)\omega \approx -2\nabla\bullet\vec{Q}\right]$ where $\vec{Q}=-\frac{R}{P}\left[\left(\frac{\partial\vec{V}_g}{\partial x}\bullet\nabla T\right)i,\left(\frac{\partial\vec{V}_g}{\partial y}\bullet\nabla T\right)j\right]$. Convergent Q-vectors then diagnose

regions where there is QG forcing of rising vertical motion. Divergent Q-vectors define areas where there is QG forcing of downward motion. Typically the Q-vector orientation in the confluent jet-entrance region is such that Q-vector convergence exists in the warm air, equatorward of the jet, and Q-vector divergence exists in the cold air, poleward of the jet. This defines a thermally direct forced ageostrophic secondary circulation (Figure 2a).

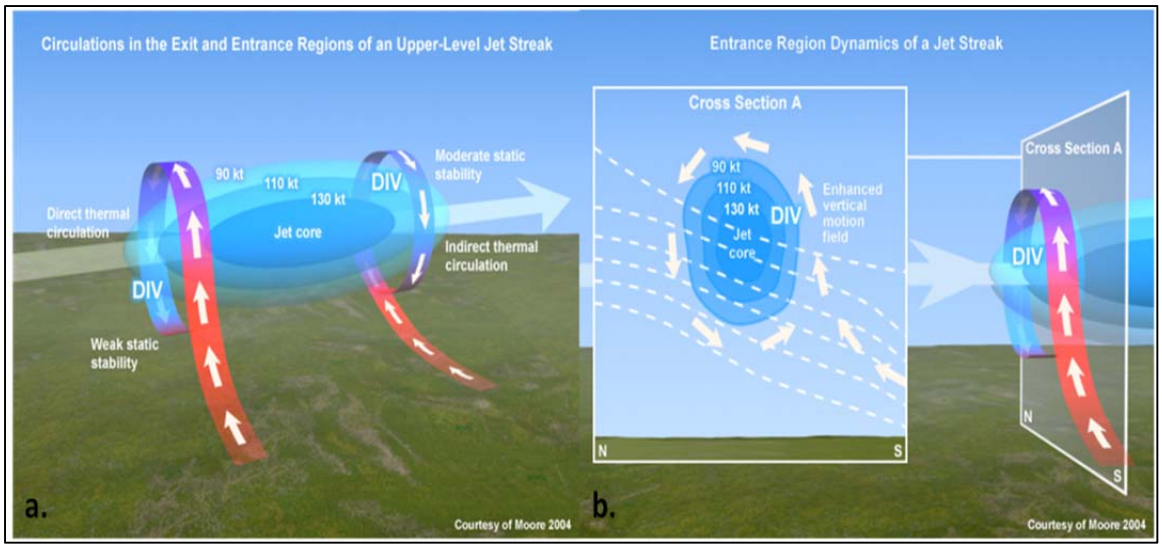


Figure 2. (a) Circulations injet-entrance and exit regions, (b) Jet-entrance region dynamics (After Moore 2004)

The adiabatic temperature changes associated with the rising and sinking branches of the ageostrophic circulation act to reduce the temperature gradient beneath the jet. The upper-level and lower-level meridional winds of the ageostrophic circulation act to increase the vertical wind shear of the geostrophic wind in the jet-entrance region. Therefore, the QG forced ageostrophic circulation acts to restore thermal wind balance on the jet-entrance region (Figure 2b). A similar but opposite oriented circulation exists at the jet exit region (Martin 2006).

Finally, the occurrence of a PRE has been defined to be associated with rainfall rates that exceed 100 mm in a 24-hour period. This threshold was established to separate the rainfall associated with PRE dynamics from rainfall resulting from isolated convective activity along frontal boundaries (Cote 2007). The increased rainfall is due to the interaction between the poleward moving high PW air of tropical origin and the

vertical ageostrophic circulation associated with the jet-entrance region. Therefore, the appropriate phasing of space and time between the system is required for PRE formation.

The potential rapid and localized combination of tropical and midlatitude factors can create a large forecasting problem for meteorologists and crisis planners for three main reasons. First, most of the attention is centered on the TC itself, which is often seen as the greater threat (Cote 2007). Second, the path and timing of the moisture plume is extremely important to PRE development and also susceptible to model error (Schumacher et al. 2010). Finally, the distance and time displacement of the moisture plume can, on average, be greater than 1000 km and 36 hours ahead of the generating TCs passing (Cote 2007).

## B. TROPICAL CYCLONE CONDITIONS OF READINESS (TCCOR)

### 1. Defining Conditions of Readiness

In efforts to consolidate and disseminate warnings for hazardous and destructive weather to the U.S. Navy Fleets as well as Navy and Maine Corps installations, in 2008 the Oceanographer of the Navy updated OPNAV Instruction 3140.24F, which includes a summary table (Table 1) of hazardous and destructive warnings and their respective originators (DON 2008). A myriad of other local command instructions reiterate and further quantify warning thresholds and procedures included in OPNAV 3140.24F, however the general structure and timeline of categories I thru V, with category I being the most severe, remains the same.

| TROPICAL CYCLONE, SUB-TROPICAL, EXTRA-TROPICAL, WIND STORMS (Issue using gale, storm, tropical storm, or hurricane/typhoon to indicate force of destructive winds.) | |
|---|---|
| Condition V | Destructive winds are possible within 96 hours. |
| Condition IV | Trend indicates a possible threat of destructive wind of the force indicated within 72 hours. Review hazardous and destructive weather implementation plans, as established by local regulations. |
| Condition III | Destructive winds of force indicated are possible within 48 hours. Take preliminary precautions. |
| Condition II | Destructive winds of the force indicated are anticipated within 24 hours. Take precautions that will permit establishment of an appropriate state of readiness on short notice. |
| Condition I | Destructive winds of the force indicated are occurring or anticipated within 12 hours. Take final precautions as prescribed. |

Table 1. U.S. Navy Conditions of Readiness (From OPNAVINST 3140.2F)

As seen in Table 1, the prefix gale, storm, tropical storm, hurricane, or typhoon can be added to the conditions of readiness to specify the forcing mechanism of the destructive winds. To consolidate the process, tropical cyclone is synonymous with hurricane and typhoon and therefore the prefix TC is commonly used by the National Hurricane Center (NHC) and the Joint Typhoon Warning Center (JTWC) when recommending TCCORs. The instruction does leave the specific precautionary measures to be taken for each level of readiness up to the local installation commander as geography, personnel readiness, and proximity to support systems varies drastically between all installations, even installations within the same region.

As will be shown, some bases by their geography are more or less susceptible to enhanced rainfall than others. By this reasoning, if precautionary measures are deemed necessary by the Oceanographer of the Navy (OOTN) for TCCORs due to high winds and storm proximity, then each local command should likewise have complete control over what precautionary steps should be taken with regards to PRE formation at or around their installation.

For comparison, the U.S. Air Force has a similar structure for Hurricane/Typhoon reporting procedures that align with the timelines listed in Table 1. Although the reporting requirements explicitly quantify destructive winds, the Air Force similarly leaves the precautionary measures to be taken up to the discretion of the local area commanders as indicated in Table 2 (DOAF 2011).

| AF OPREP-3 Hurricane/Tropical Cyclone (Typhoon) Conditions of Readiness (HURCON/TCCOR) | |
|---|---|
| HURCON 5 | Automatic state of preparedness initiated on 1 June of each year. NOTE: There is no TCCOR 5 |
| HURCON/TCCOR 4 | 72 hours prior to possible arrival of sustained 50 KT/58 MPH winds. |
| HURCON/TCCOR 3 | 48 hours prior to possible arrival of sustained 50 KT/58 MPH winds. |
| HURCON/TCCOR 2 | 24 hours prior to possible arrival of sustained 50 KT/58 MPH winds. |
| HURCON/TCCOR 1 | 12 hours prior to possible arrival of sustained 50 KT/58 MPH winds. |

Table 2. U.S. Air Force OPREP-3 reporting requirements (From AF 10-206)

### 2. Setting Tropical Cyclone Conditions of Readiness

In efforts to consolidate, disseminate, and improve the warnings for hazardous and destructive weather to the U.S. military forces a comprehensive summary of the TCCOR recommendation process for four very different installations within U.S. Forces Japan was conducted by Wallace (2008). The readiness recommendation process begins after the TC has been confirmed and the forecast track and forecast storm development has been defined (Wallace 2008). When TC's are being tracked by JTWC (Pacific) or NHC (Atlantic), each respective center conducts regular teleconference calls for all interested personnel across the DoD and local weather affiliates. The local base commanders or weather centers attend these conference calls in which mesoscale influence, forecast, and TCCOR initiation and updates are often discussed. When the TC track and storm strength is forecasted to fall within one of the thresholds in Table 1, the warning center (JTWC or NHC) will make a recommendation to the local weather commands for establishing a TCCOR warning. The local weather commands then have the duty to recommend to their regional commands, or local TCCOR authorities, a

readiness condition. When initiated by the regional commands this TCCOR becomes the minimum level of readiness to be adhered to for all local bases within the region under their purview (Wallace 2008).

When initiated, the proposed TCCOR readiness is established with specific required actions outlined per individual command standard operating procedures. However, the local base commander is given leeway to place their respective command into a more restrictive TCCOR than the issuing authority with the only stipulation being that the TCCOR can never be relaxed below the issuing authorities level (DON 2008). An example of this is that Okinawa is placed into a permanent TCCOR IV state at the beginning of the TC season and does not relax that until the end of the TC season. This is done because of Okinawa's proximity to historical TC formation sites, arguing that if a TC forms in the Pacific Okinawa will already be within the category IV threshold and therefore should remain there throughout the season (CNFJ 2010). Other installations such as Fleet Activities Sasebo and Misawa AB, which are not within the TC formation danger zone, have different TCCOR warning processes.

#### *a. Fleet Activities Sasebo*

Fleet Activities Sasebo is located on the island of Kyushu just southwest of the island of Honshu, in the Nagasaki Prefecture, approximately 1200 km west of Tokyo (Figure 3). Fleet Activities Sasebo is homeport to 10 ships, which are part of the United States Forward Deployed Naval Force, and are accompanied in Japan by over 6,000 military support members and families.

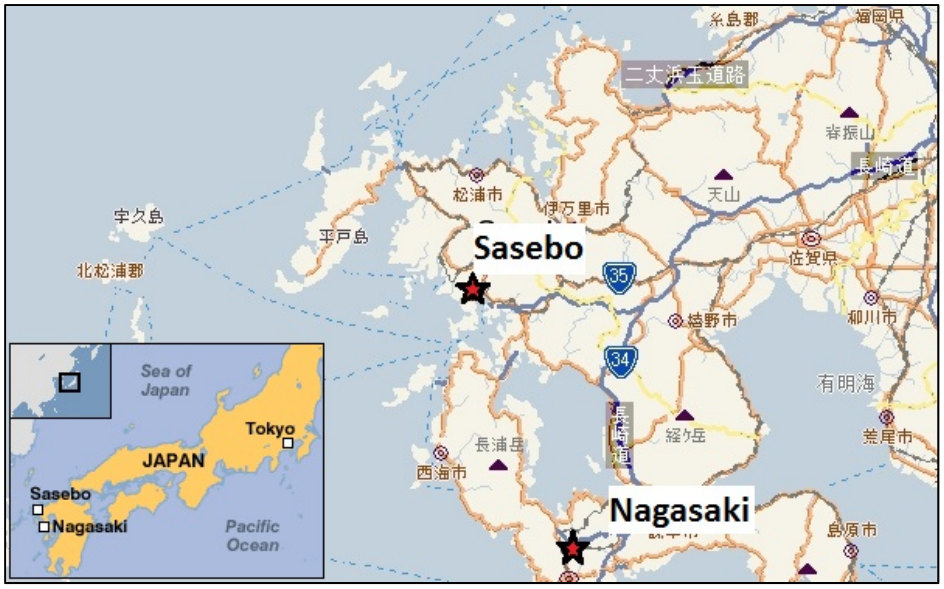


Figure 3. Graphical depiction the Nagasaki Prefecture Region around Sasebo (After http://www.weather-forecast.com/locations/Sasebo)

Sasebo has long been considered a typhoon "safe haven" by the Navy given its immediate geography. Sasebo is a deep water port surrounded on all sides by hills with no direct frontage to the Pacific Ocean. The Port of Sasebo is bordered to the southwest by the Philippine Sea and to the west by the East China Sea. Sasebo is also sheltered by way of Kyushu Island from the Pacific Ocean and therefore has long been considered a safe haven for most sea going vessels in the Pacific, not just U.S. warships (NRL 2009).

In accordance with PACOMINST 0539.1, Commander U.S. Forces Japan (USFJ) is the TCCOR authority for all U.S. military and DoD commands and installations within the Japanese archipelago. The USFJ has delegated TCCOR authority for Fleet Activities Sasebo and Yokosuka to Commander, Naval Forces Japan (CNFJ) who receives recommendations from the Navy Oceanographic and Antisubmarine Warfare Center (NOAC), Yokosuka (CNFJ 2010). As stated before, NOAC Yokosuka is in direct and constant communications with the JTWC, in efforts to maintain the most accurate TC forecast available at all times in hopes to make the best TCCOR recommendations (Table 3) at all times.

During the duration of TC Roke, TCCOR ALL CLEAR remained in effect for Fleet Activities Sasebo, which is to be expected given their relative position to the storm track and the current foul weather instructions within the region.

| Commander Naval Oceanographic Antisubmarine Warfare Center Commanding Officer's SOP | |
|---|---|
| TCCOR 4 | Trend indicates a possible threat of destructive winds within 72 hours. |
| TCCOR 3 | Destructive winds are possible within 48 hours. |
| TCCOR 2 | Destructive winds are anticipated within 24 hours. *Initial TCCOR meeting with Tenant and Fleet representation, 48 to 72 hours from forecast tropical cyclone CPA.* |
| TCCOR 1 | Destructive winds are anticipated within 12 hours. |
| TCCOR 1 "CAUTION" | Damaging winds with frequent gusts of 50-59 knots are occurring. |
| TCCOR 1 "EMERGENCY" | Destructive winds or gusts 60 knots or greater are occurring. |
| TCCOR "RECOVERY" | Destructive winds no longer forecast to occur. |
| TCCOR "ALL CLEAR" | The threat of severe weather associated with the Tropical Cyclone is over. |
| "STORM WATCH" | The tropical cyclone is expected to pass dangerously close to the installation and any shift in track or increase in intensity may result in rapid elevation in CORs and destructive force winds occurring on short notice. At a minimum, damaging winds may be experienced when this condition is set. |
| Damaging Winds: Sustained winds 34-49 knots (40-56 mph), or frequent gusts of 40-59 knots (46-68 mph) are forecast to occur. (Same criteria for GALE Warning) | |
| Destructive Winds: Sustained winds 50 knots (58 mph) or greater or frequent gusts of 60 knots (69 mph) or greater are forecast to occur. (Same criteria for STORM Warning) | |

Table 3. NOAC, Yokosuka TCCOR thresholds (From Commander NOAC, Yokosuka SOP)

It should be noted that Commander Fleet Activities Sasebo has the authority to reject NOAC Yokosuka recommended TCCOR however must notify CNFJ regional operations center if he chooses to do so. Furthermore FAS hazardous and destructive weather plan, similar to other installations, defines TCCOR by only the

magnitude of and proximity to destructive winds. Fleet Activity Sasebo does differ slightly in that they identify two additional warning criteria for thunderstorms, T1 and T2 (Table 4). These T1 and T2 warnings are also recommended by NOAC Yokosuka (CFAS 2010).

| Commander, Fleet Activities Sasebo Hazardous and Destructive Weather Plan | |
|---|---|
| Thunderstorm Advisory (T2) | Destructive winds and accompanying thunderstorms are within 25 Nautical Miles (NM). Or expected within 6 hours. Associated lighting/thunder, torrential rain, hail, severe downbursts and sudden wind shifts are possible. Take precautions that will permit establishment of an appropriate state of readiness on short notice. |
| Thunderstorm Warning (T1) | Destructive winds and accompanying thunderstorms are within 10 Nautical Miles (NM). Or expected within 1 hour. Associated lighting/thunder, torrential rain, hail, severe downbursts and sudden wind shifts are possible. Take immediate safety precautions and shelter. |

Table 4. Fleet Activities Sasebo Thunderstorm Warning Criteria (From Commander, Fleet Activities Sasebo 2010)

### *b. Misawa Air Base*

Misawa AB is located on the northeastern side of the island of Honshu, in the Aomori Prefecture, approximately 700 km north of Tokyo (Figure 4). Misawa AB is a joint command and home to all four military services via the Air Force 35th Fighter Wing, the Naval Air Facility Misawa, Company I Marine Support Battalion, and the Army's 403rd Military Intelligence Detachment. In total Misawa AB is home to approximately 10,000 U.S. military, support personnel, and families and one of the only true joint operating bases within the region.


Figure 4. Graphical depiction Aomori Prefecture containing Misawa and Aomori (After http://www.weather-forecast.com/locations/Misawa)

Similar in doctrine to the U.S. Navy, Misawa AB's 35th Fighter Wing Commander is the TCCOR authority for Misawa and the Hachinone Petroleum, Oil and Lubricants Depot. Misawa AB Commander receives recommendations from the 35th Operations Support Squadron who works directly with U.S. Forces Japan and JTWC to receive updates on all TC forecasts and TCCOR changes for the island of Honshu.

THIS PAGE INTENTIONALLY LEFT BLANK

# III. METHODOLOGY

## A. DATA

Data analyzed in this thesis came from a variety of open sources and research communities. The time period of 13–24 September 2011 is analyzed. This period begins just after Roke reached TC status to just after the storm passed the main Japanese Island of Honshu.

### 1. Satellite Imagery

Color enhanced infrared and water vapor satellite imagery (Figure 5), were collected open source from the National Oceanographic and Atmospheric Administration's (NOAA) portal to METSAT-2 at 3-h intervals over the entire Eastern Hemisphere. Using these images, it was possible to localize the position and motion of TC Roke as well as to help identify and track the background weather patterns over Asia and the Pacific Ocean.

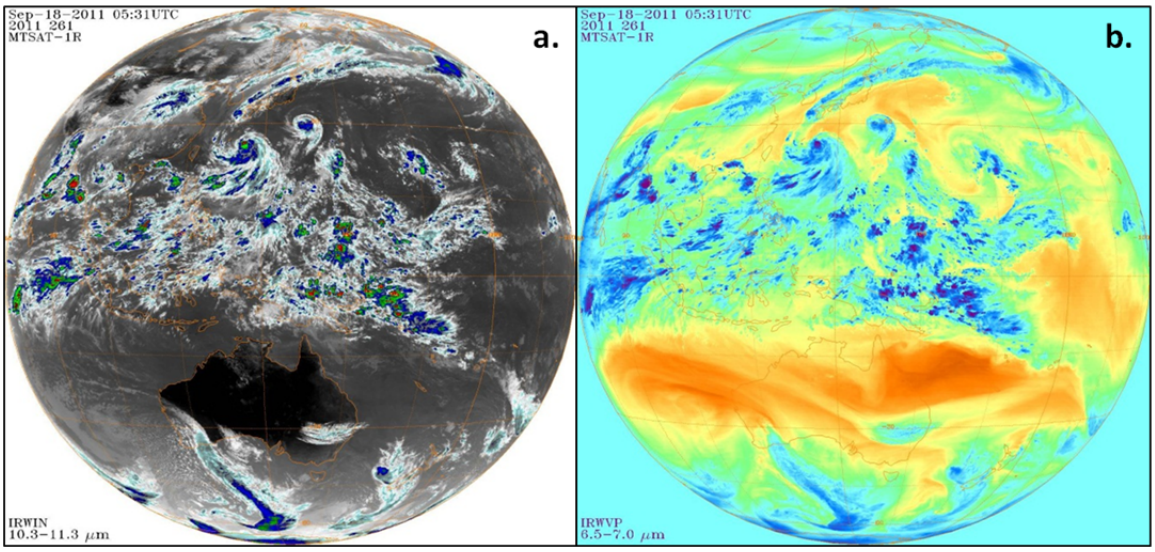


Figure 5. (a) Color enhanced METSAT-2 full disk infrared (IR) and (b) color enhanced METSAT-2 full disk water vapor for 0531 UTC 18 September 2011 over the Eastern Hemisphere (From http://www.ncdc.noaa.gov/)

Additional archived satellite images (Figure 6) were collected from the Naval Research Laboratory, Monterey (NRLMRY) to examine the specific area of interest.

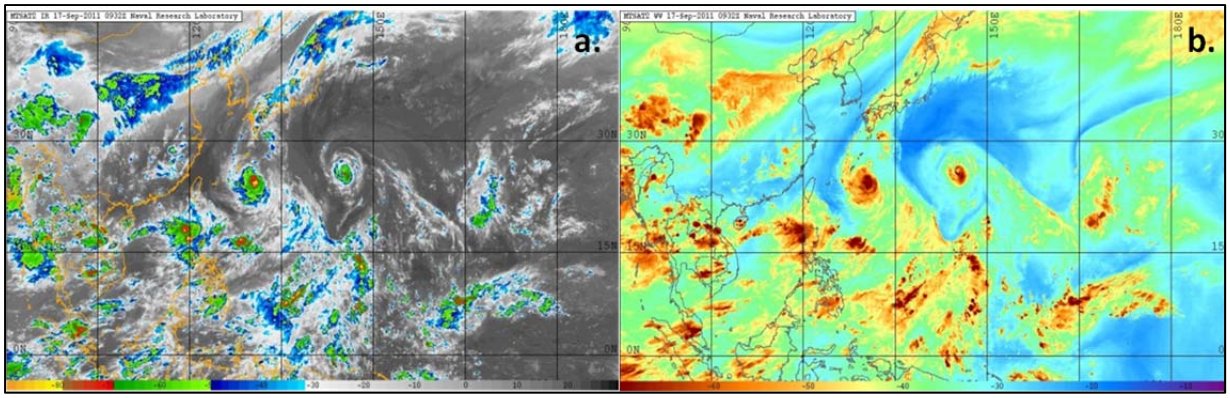


Figure 6. (a) METSAT-2 color enhanced IR imagery and (b) color enhanced water vapor imagery at 0932 UTC 17 September 2011 (from NRLMRY)

The NRLMRY blended geostationary microwave rain rate product (Figure 7) was utilized to capture 1, 3, 6, and 24-h blended rainfall accumulations to augment autonomous rainfall gauge reporting data.

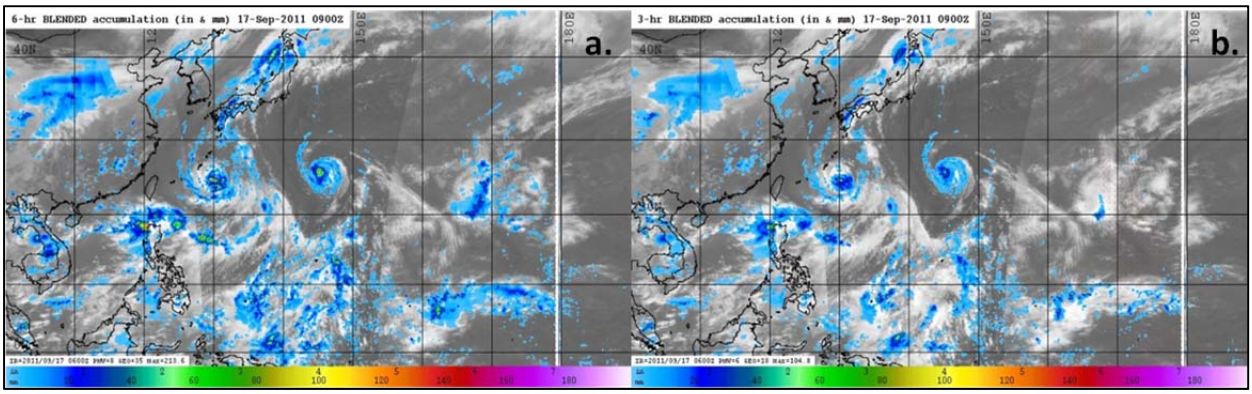


Figure 7. (a) Blended 3-h rain accumulations and (b) blended 6-h rain accumulations at 0900 UTC 17 September 2011 (From NRLMRY)

## 2. Rainfall Data

Utilizing the 24-h rainfall accumulation satellite imagery, it was possible to identify specific areas within the Japanese archipelago that would have been subject to the 100 mm 24 $h^{-1}$ PRE threshold. Next, the precipitation data for major townships and cities within the regions were obtained via the National Climatic Data Center (NCDC) record of global integrated hourly surface data archives. These data were used to define locations that met the specific PRE threshold of 100 mm per 24-h (Table 5).

| | Max 24-h PRE Rainfall (mm 24 $h^{-1}$) | Total PRE Rainfall (mm) | PRE Time (DD/UTC) | TC Roke Max Rainfall (mm 24 $h^{-1}$) | Total TC Roke Rainfall (mm) | TC Roke Time (DD/UTC) |
|---|---|---|---|---|---|---|
| **Nagasaki** | **110** | **112** | **18/0000** | **0** | **0** | **N/A** |
| **Nagoya** | **9** | **9** | **17/0000** | **97** | **275** | **20/1200** |
| **Yokohama** | **7** | **7** | **17/0000** | **168** | **194** | **21/0000** |
| **Tokyo** | **6** | **6** | **17/0000** | **146** | **176** | **21/0000** |
| **Morioka** | **39** | **44** | **18/0000** | **87** | **143** | **21/1200** |
| **Misawa** | **84** | **124** | **18/0000** | **82** | **127** | **22/0000** |
| **Aomori** | **98** | **169** | **18/1200** | **78** | **107** | **22/0000** |
| **Mutsu** | **68** | **101** | **18/0000** | **41** | **49** | **21/1200** |

Table 5. Max 24-h vs. Total accumulated rainfall for PRE and TC Roke

Utilizing the NCDC data, a histogram for each city was created with accumulated rainfall in 12-h bins (Figure 8). The histograms were then examined to determine if a bimodal distribution of rainfall occurred, which would be representative of a PRE and later passage of a tropical cyclone.

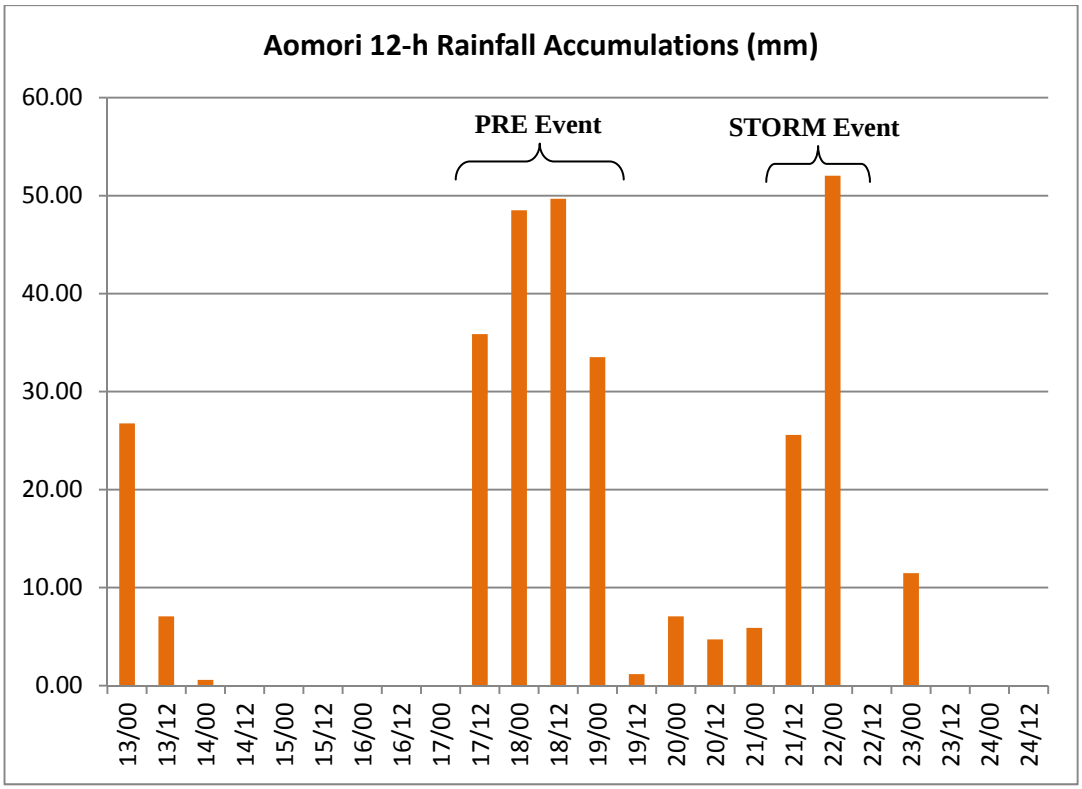


Figure 8. Aomori rainfall histogram with 12-h bin size for 0000 UTC 13 September 2011 through 1200 UTC 24 September 2011

### 3. TCCOR Data

Due to differences in the TCCOR procedures between the TCCOR authorities, the mission differences between the U.S. Air Force and U.S. Navy, and base geography and locations, the TCCOR timeline (Figure 9) for local commands within U.S. Forces Japan (USFJ) vary significantly.

To start collecting the TCCOR timeline data, it was easiest to start with Stars and Stripes military news affiliate, which has open source real-time and archived data. Stars and Stripes provided a baseline TCCOR timeline for reference for most of the installations with Japan. Stars and Stripes relay the TCCOR updates as they received them from each installation public affairs office and posted them to their website for public access. Further warnings were reiterated via the local Armed Forces Network and the U.S. Embassy in Japan, but all warnings and TCCOR updates were within the same timeline extrapolated from the Stars and Stripes bulletins.

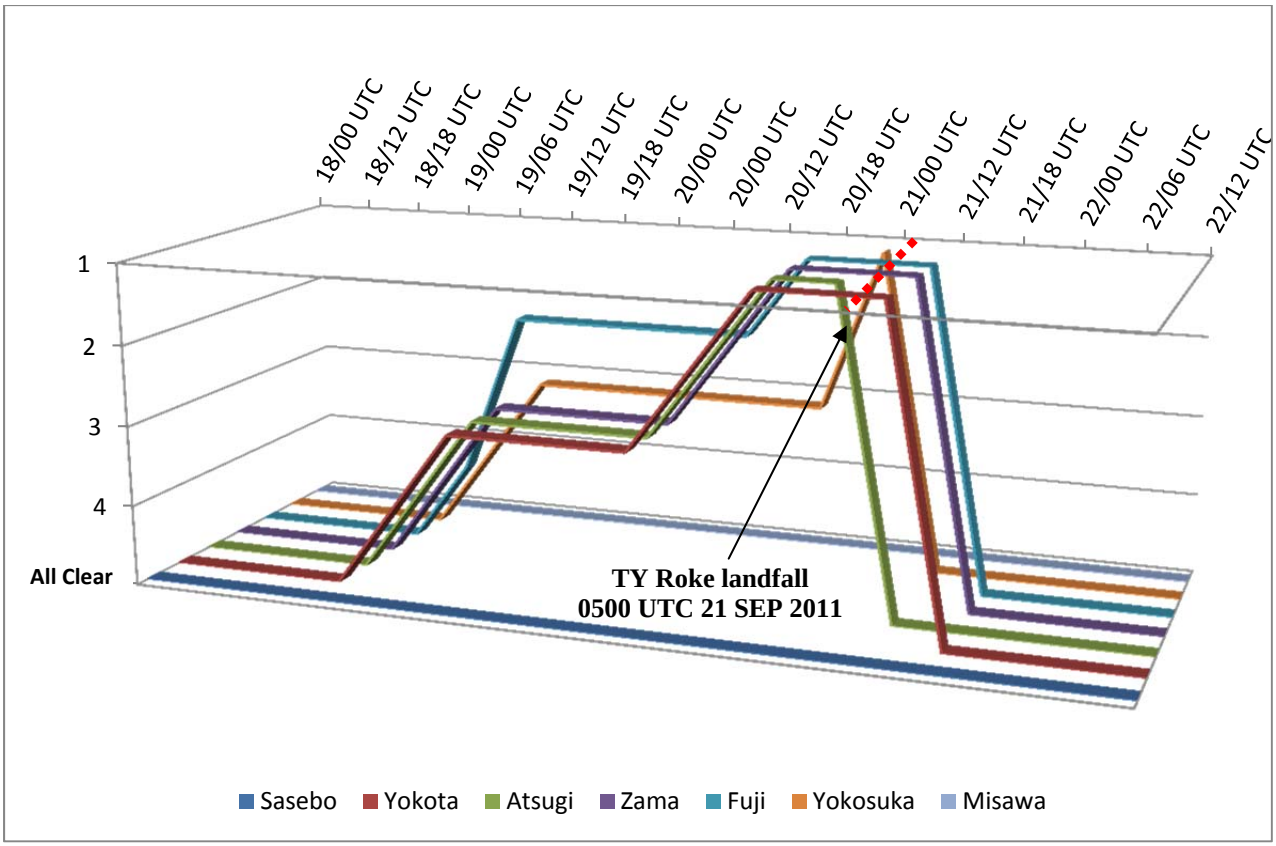


Figure 9. TY Roke TCCOR timeline showing DoD TCCOR posture with respect to TY Roke landfall (red dashed line) for military installations within USFJ

Local TCCOR authorities confirmed the Stars and Stripes TCCOR timeline for the two installations of interest. For FAS, the TCCOR timeline was confirmed by NOAC Yokosuka, which made no recommendations to the Navy TCCOR authority Commander Fleet Activities Sasebo. Further confirmation from FAS Operations Staff confirmed that no T1 or T2 warnings or local TCCORs were given Misawa AB TCCOR timeline was confirmed by 35th Operations Support Squadron, which made the recommendations to the AB 35th Fighter Wing Commander (TCCOR authority for Misawa AB).

## 4. Tropical Cyclone Roke Track Data

The best-track information for TY Roke was obtained from NOAC Yokosuka after consolidation and presentation of their tropical cyclone after action report to Commander Naval Forces Japan on 29 September 2011. Satellite archives and both

Global Forecasting System (GFS) and Weather Research and Forecasting (WRF) model simulations are used to examine the environmental conditions along the best-track.

TC Roke was first identified as a Tropical Cyclone Formation Area (TCFA) 18W by JTWC at 1800 UTC 10 September 2011 (Figure 10). The TCFA was oriented along a track directed toward the northwest and the disturbance was moving at approximately 12 kt.

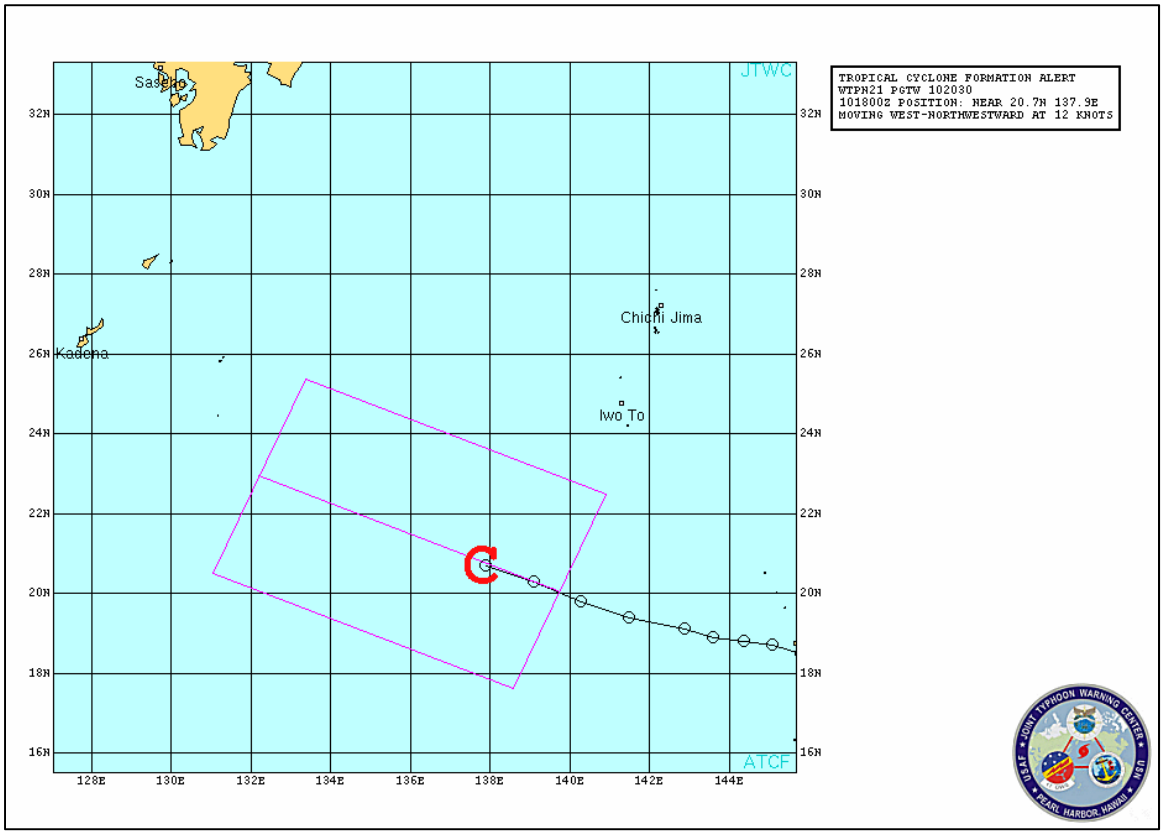


Figure 10. The TCFA graphic for 1800 UTC 10 September 2011 (From JTWC)

The 18W disturbance was then upgraded to tropical depression (TD) 18W by JTWC at 1200 UTC 11 September 2011. At this time, Roke was forecast to move toward the East China Sea (Figure 11), due to a strong subtropical ridge (not shown) that was just north of the TD. The TD reached tropical storm (TS) strength at 1800 UTC 13 September 2011 and was given the name Roke. At this time, the subtropical ridge began to move to the east as the approaching short wave upper-troposphere trough moved in from the east. The movement to the northeast was short-lived as Roke turned back to the

northwest as the ridge re-intensified. On 16 September 2011 an approaching upper-level trough from the west again weakened the ridge and the weak steering flow resulted Roke performing a cyclonic loop just east of Okinawa (Figure 11). After the loop, Roke began to recurve to the northeast towards Japan on 19 September 2011. TS Roke reached typhoon strength at 1200 UTC 19 September 2011, before making landfall on the main Japanese island of Honshu near Hamamatsu, Japan at 0500 UTC 21 September 2011 (Figure 11).

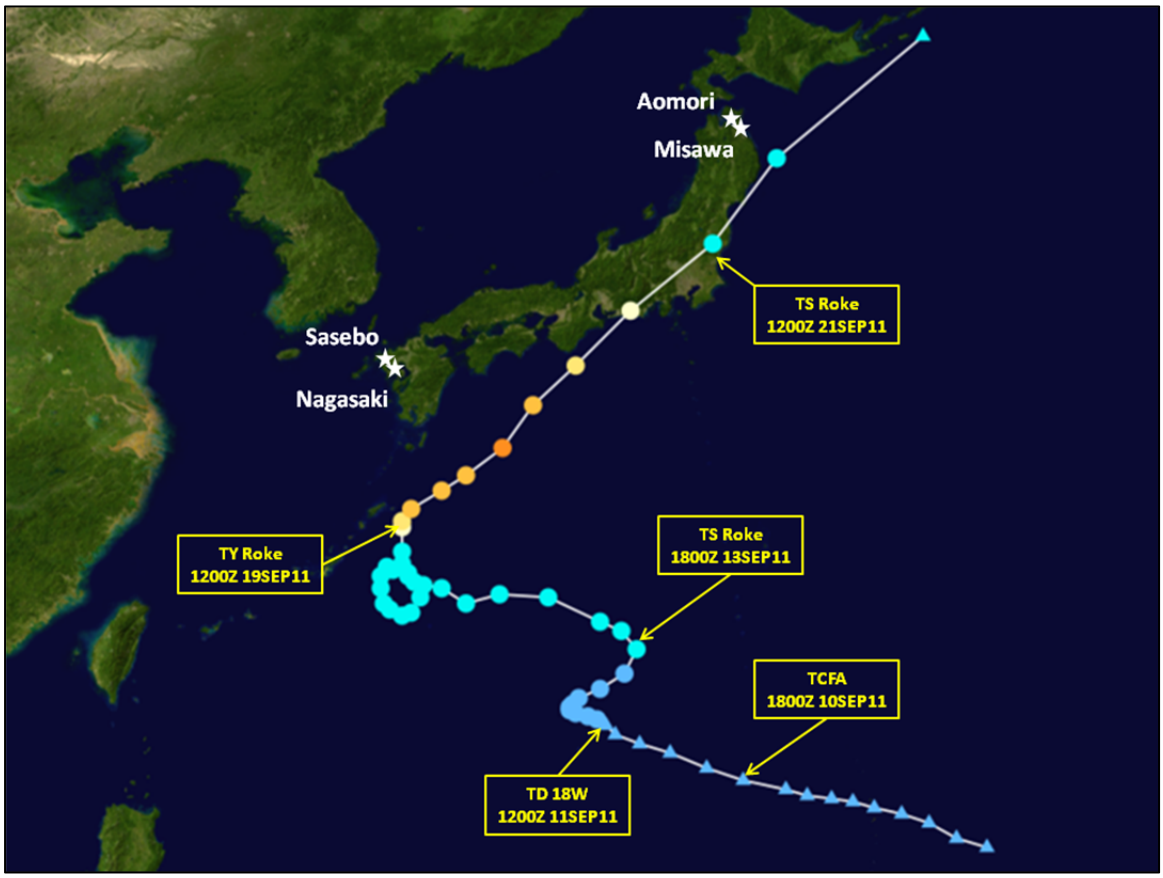


Figure 11. Typhoon Roke best track analysis (After http://en.wikipedia.org/wiki/File:Roke_2011_track.png)

After making landfall, TY Roke continued to move northeastward and satellite imagery indicated rapidly decreasing deep convection surrounding the cyclone. TY Roke followed the northeast track parallel to the Japanese islands before weakening to a TS on 1200 UTC 21 September 2011 and undergoing extratropical transition northeast of Japan.

## B. MODEL SIMULATION

### 1. Global Forecasting System (GFS) Model

Analyses for the GFS (0.5 degree resolution), which is the operational global numerical forecast model at the National Center for Environmental Prediction (NCEP), were utilized to examine the large-scale environment over the North Pacific and East Asia during the period of TY Roke. The parameters of height, winds, temperature, and precipitable water (PW) were examined (Figure 12).

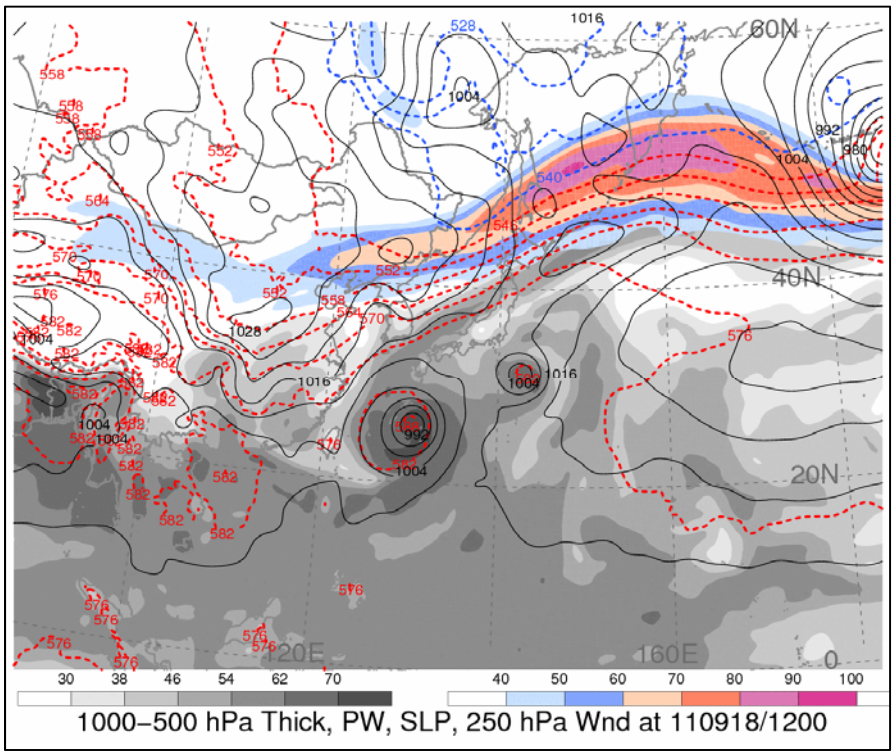


Figure 12. Analyzed GFS fields of precipitable water (shaded in mm), sea-level pressure (solid black line in hPA), and 1000-500 hPA thickness (red dashed line in dam) for 1200 UTC 18 September 2011 (From http://www.atmos.albany.edu/student/heathera/slp_thick/wpac/7_to_22_sep.html)

Additionally, various diagnostic quantities (i.e. dynamic tropopause and quasi-geostrophic forcing of vertical motion) are computed with the GFS analysis in attempts to locate the specific antecedent dynamics associated with PRE development (Figure 13).

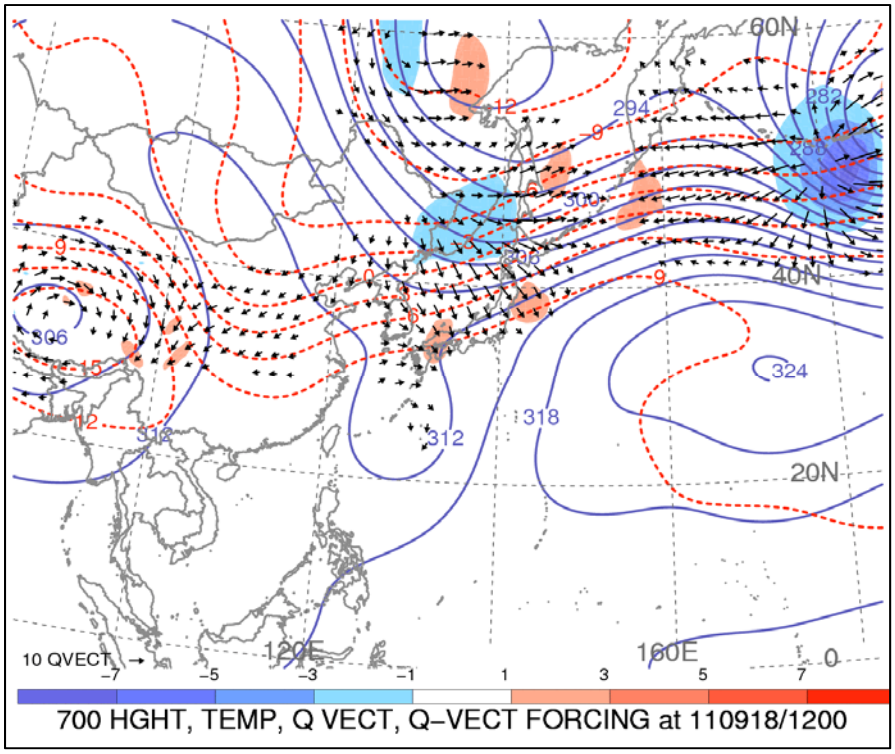


Figure 13. Analyzed GFS field of 700 hPa height contour (dam), Q-vector (scale at lower left in units $10^{-7}$ Pa $m^{-1}$ $s^{-1}$), and quasi-geostrophic forcing of vertical motion (shaded in units of $10^{-12}$ Pa $m^{-2}$ $s^{-1}$) for 1200 UTC 18 September 2011 (From http://www.atmos.albany.edu/student/heathera/qvect/wpac/7_to_22_sep.html)

## 2. Weather Research and Forecasting (WRF) Model

The WRF model is widely used by researchers to perform model simulations using real data or idealized initial conditions. Analyses and forecast fields from the WRF model were utilized to examine the regional environment over the Japan archipelago during TY Roke. Along with analyses and forecast of height, winds, temperature, and PW, WRF-based rainfall accumulations for specific geographic locations were analyzed.

The WRF was run using a 27 km static outer domain with a 60 s time step and a nested 9 km static inner domain with a 20 s time step (Figure 14). The inner domain was centered over the Japan archipelago. Boundary conditions for WRF were generated using the GFS analysis for the analyzed periods.

The WRF model was run using the WRF single-moment (WSM) 6-class graupel microphysics package and the Betts-Miller-Janjic cloud physics package as well as the Yonsei University (YSU) planetary boundary layer (PBL) scheme.

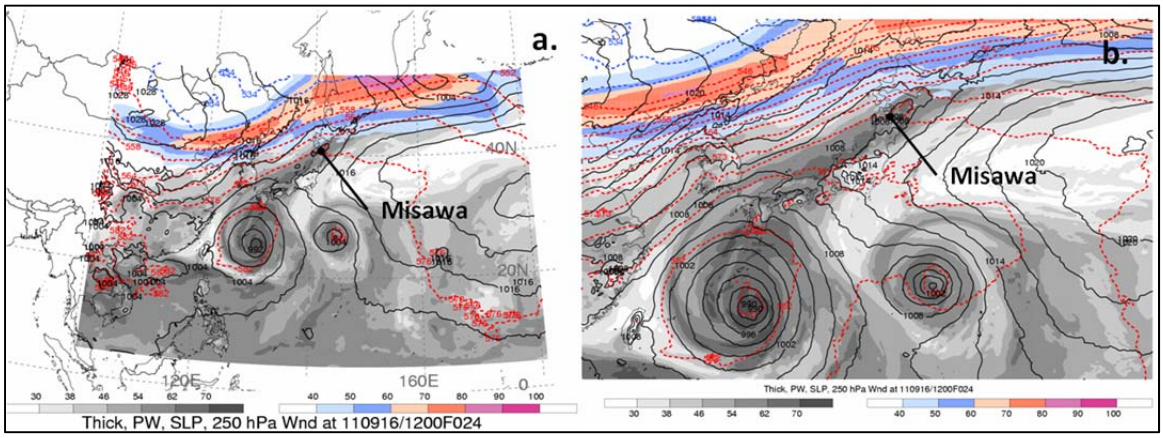


Figure 14. (a) WRF 27-km forecast and (b) WRF 9-km forecast of precipitable water (shaded in mm), sea-level pressure (solid black line in hPA), and 1000–500 hPA thickness (red dashed line in dam) for 1200 UTC 17 September 2011 (After http://www.met.nps.edu/~hmarcham/roke/)

Two WRF simulations were conducted. The first was centered in time to contain the Misawa PRE. This simulation begins at 1200 UTC 16 September 2011 and runs through 1200 UTC 22 September 2011. This time period captures the actual PRE event at Misawa as well as the significant rain event recorded at Nagasaki. The second WRF model simulation begins at 1200 UTC 19 September 2011 and runs through 1200 UTC 24 September 2011 and is centered on the rain event associated with TY Roke passage at its CPA to Misawa.

## 3. Model Characteristics

The GFS analyses were in good agreement with satellite imagery, radar imagery, and JMA best track data available for the time period between 14–24 September 2011 with respect to TC Roke itself. After approximately 72 h the WRF model simulations begin to deviate from JMA best track analyses. after approximately 72 h in synoptic development and timing. This led to creation of two model forecast simulations. The first WRF model run (WRF-1) was initialized at 1200 UTC 16 September 2011 and ran

through 1200 UTC 22 September 2011 and was intended to capture the Misawa PRE. The second WRF model run (WRF-2) was initialized at 1200 UTC 19 September 2011 and ran through 1200 UTC 24 September 2011 and was intended to capture the Misawa rain event associated directly with Roke's passage at CPA (Table 5). Each simulation was designed to allow for a 24-h run time prior to the onset of each event and plotted for comparison against both GFS and JMA best track data (Figure 15).

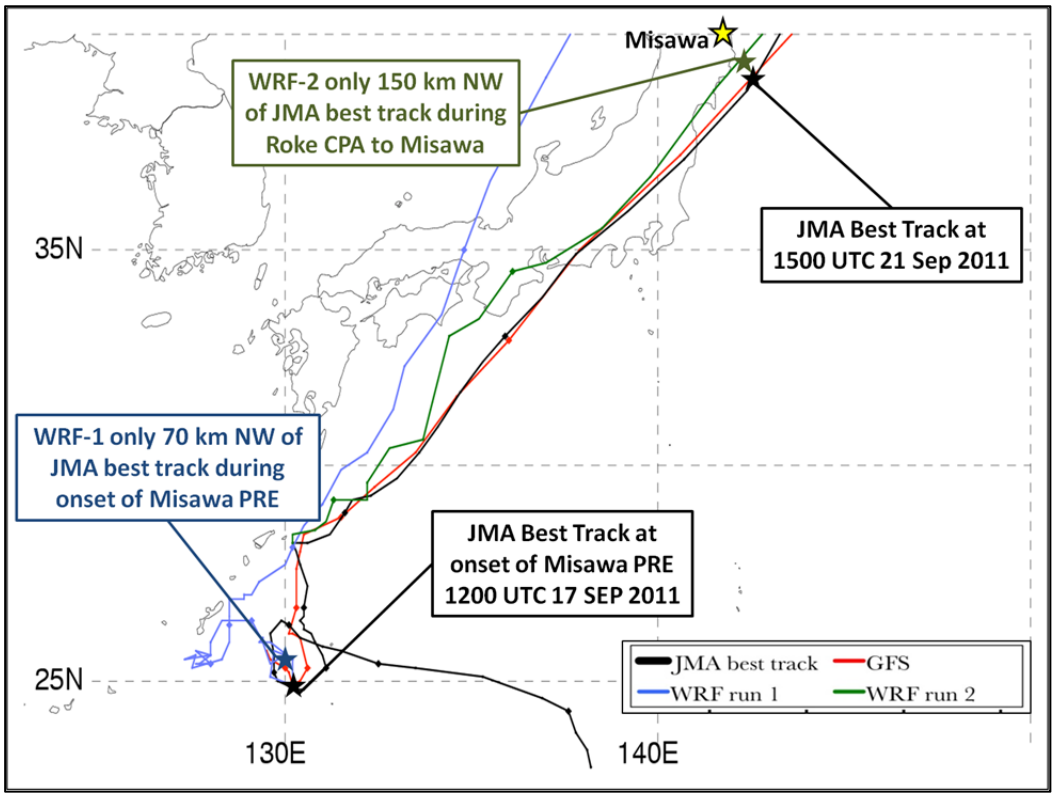


Figure 15. TC Roke track comparison of JMA best track (black line), GFS (0.5 deg.) analyses (red line), WRF (27-km) forecast track 1 from 1200 UTC 16 September 2011 through 1200 UTC 22 September 2011 (blue line), and WRF (27-km) forecast track 2 from 1200 UTC 19 September 2011 through 1200 UTC 24 September 2011 (green line) where diamonds denote 0000 UTC times and dots denote 0600, 1200, and 1800 UTC times (After http://www.met.nps.edu/~hmarcham/roke/)

In WRF-1 Roke to performed two cyclone loops east of Okinawa compared to the one cyclone loop actually followed by Roke (Figure 15). The WRF-1 forecast track crosses over the Japan archipelago and into the Sea of Japan where the JMA best track recurves quicker and passes just east of Japan on the 21 September 2011. Because

WRF-1 was initialized only 24-h prior to the Misawa PRE, it is displaced only 70 km northwest of JMA best track at 1200 UTC 17 September 2011 (Figure 15), which is the time of the PRE over Misawa. The WRF-2 forecast track of Roke is in much better spatial and temporal agreement with JMA best track. Only a 150 km displacement difference exists between the tracks during the time of closest approach of Roke at 1500 UTC 21 September 2011 (Figure 15). The relatively small spatial differences between the WRF and JMA best track during their respective rain events provides us with some confidence in the WRF simulations to represent the overall atmospheric conditions.

In terms of forecast intensity, the GFS analyses were not in good agreement with JMA best track data (Figure 16).

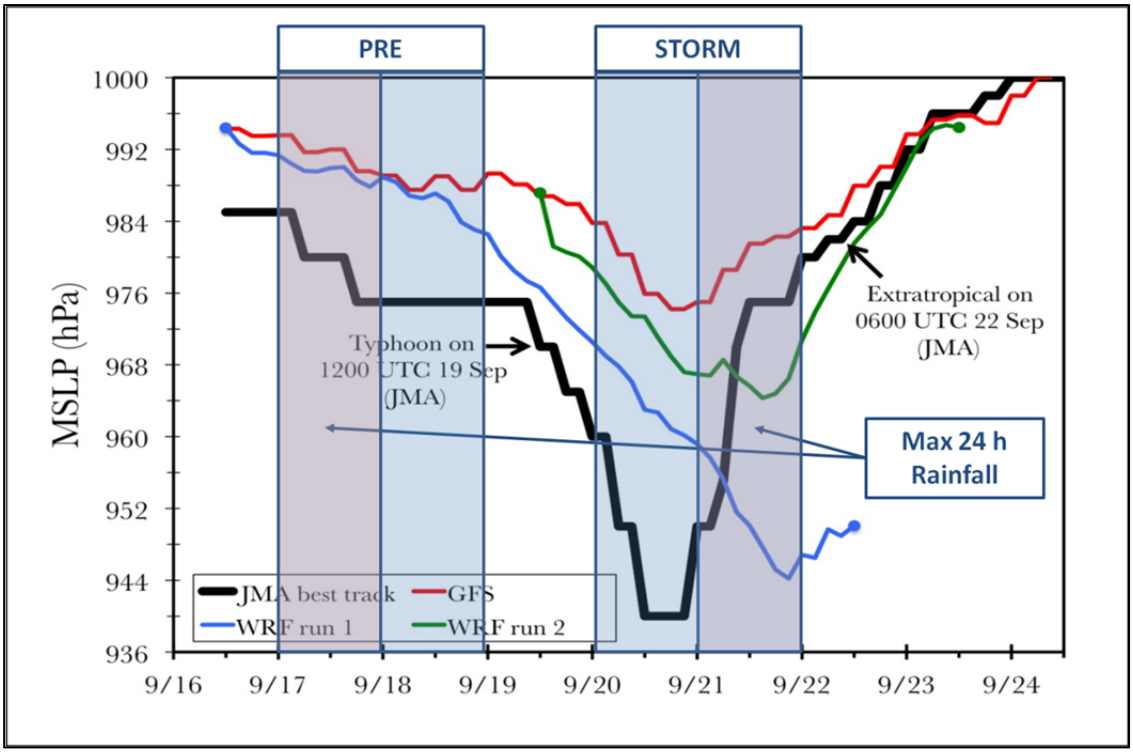


Figure 16. TC Roke MSLP Comparison of JMA best track (black line), GFS (0.5 deg.) analyses (red line), WRF (27-km) forecast track 1 from 1200 UTC 16 September 2011 through 1200 UTC 22 September 2011 (blue line), and WRF (27-km) forecast track 2 from 1200 UTC 19 September 2011 through 1200 UTC 24 September 2011 (green line), shaded rain events PRE(STORM) on left(right) with max 24 h rain period shaded in red (After http://www.met.nps.edu/~hmarcham/roke/)

Similarly, the WRF simulations did not do a much better job of either deepening or weakening of TC Roke when compared to JMA best track data. By highlighting the separate rain event time periods (Figure 16) , as well as the maximum 24 h rainfall period embedded during each rain event, it is determined that on a relative scale the WRF simulations provide a better representation of overall atmospheric conditions than the than GFS analyses when compared to JMA best track MSLP.

THIS PAGE INTENTIONALLY LEFT BLANK

# IV. ANALYSIS AND RESULTS

## A. MISAWA PREDECESSOR RAIN EVENT

Misawa AB began experiencing heavy rainfall at 0000 UTC 17 September 2011 (Figure 17) and the rain continued for two days through 0000 UTC 19 September 2011. The two day cumulative rainfall was 124 mm (4.88 in.).

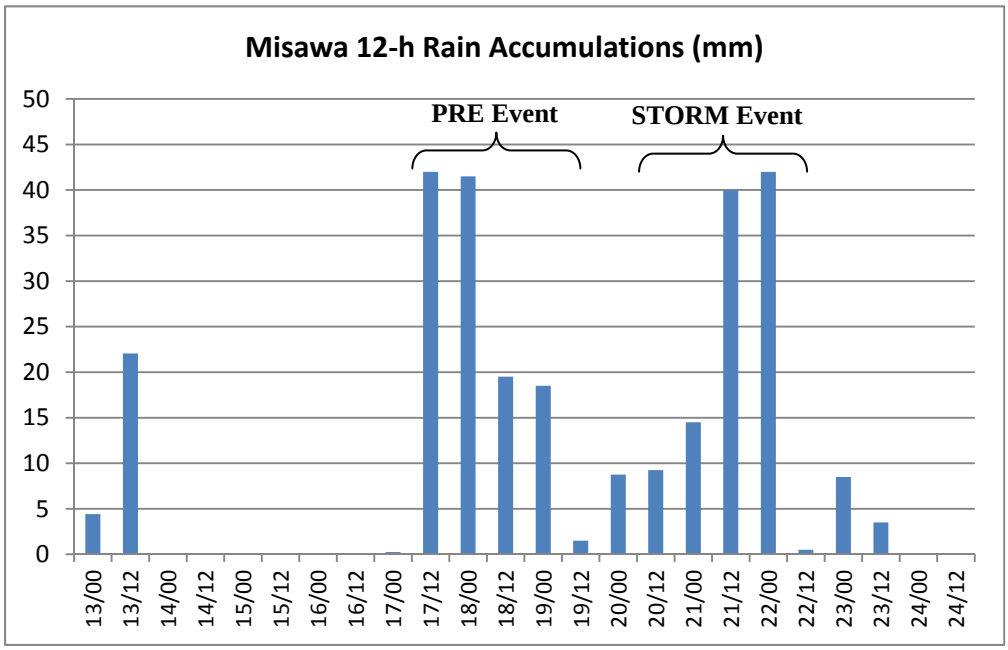


Figure 17. Misawa rainfall histogram with 12-h bin size for 0000 UTC 13 September 2011 through 1200 UTC 24 September 2011 collected from NCDC

Further analysis of Figure 17 identifies a clear bimodal rainfall accumulation pattern over Misawa AB, which is specific signature of a left of track (LOT) PRE rainfall event associated with recurving TCs. The first rainfall peak is due to the PRE while the second event is related to the passage of the TC near Misawa. The maximum 24-h PRE rainfall occurs a full 4 days ahead of the maximum 24-h storm rain event.

### 1. Rainfall Analysis

The maximum 24-h rainfall of 84 mm (3.31 in.) occurred in the first 24-h period of the two-day event between 0000 UTC 17 September 2011 through 0000 UTC on 18

September 2011 (Figure 17). The measured 84 mm 24 $h^{-1}$ does not meet the strict threshold of 100 mm 24 $h^{-1}$ set by Cote (2007). Because the NCDC observation station at Misawa AB contains 12-h cumulative rainfall, and a significant amount of rain occurred in the following 12-h, it is possible that the strict 100 mm 24 $h^{-1}$ threshold was met, but not autonomously recorded as such.

Radar data collected between 17–18 September 2011 (Figure 18) define the character and intensity of precipitation during this first rain event at Misawa. Analysis of the radar imagery indicates that light rain (< 1 mm $h^{-1}$) was falling at 0000 UTC 17 September 2011 (Figure 18a). Rainfall intensity increased along a region that was oriented from the southwest to northeast (Figure 18b). At 1200 UTC 17 September 2011, relatively heavy rainfall (16–32 mm $h^{-1}$) occurred. Medium intensity (8–16 mm $h^{-1}$) rain continued to fall through 1200 UTC 18 September 2011 (Figures 18c,d). Therefore, if hourly cumulative data were available for the period, it is likely that a specific 24-h period exists in which the 100 mm 24 $h^{-1}$ criterion was met.

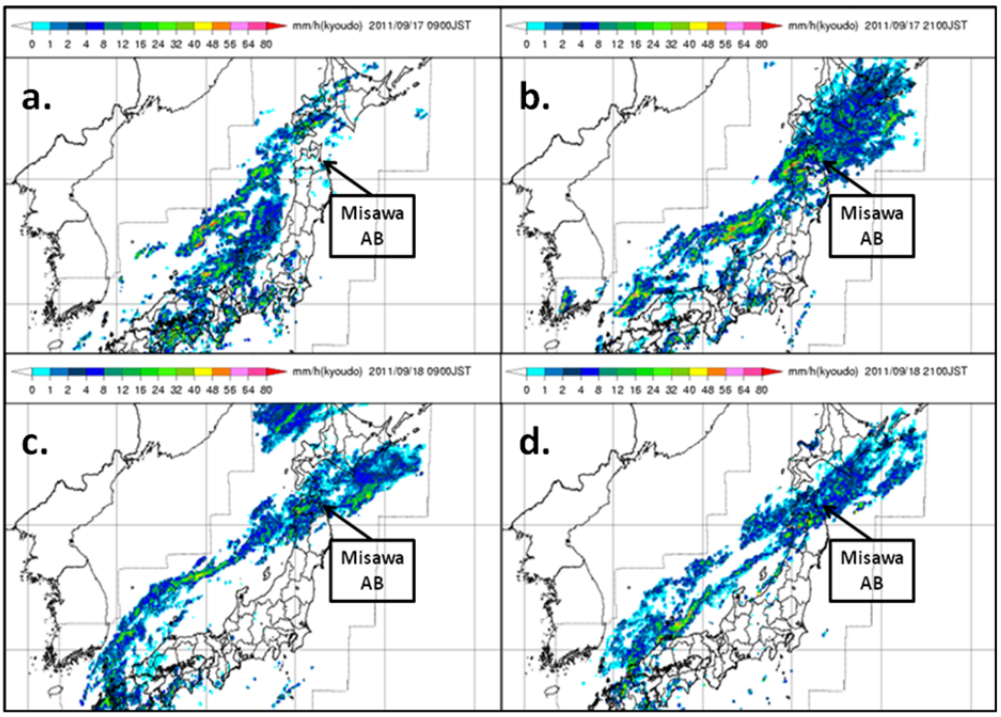


Figure 18. Radar derived hourly rain rates (mm $h^{-1}$) for (a) 0000 UTC 17 September 2011, (b) 1200 UTC 17 September 2011, (c) 0000 UTC 18 September 2011, (d) 1200 18 September 2011 (After JMA)

Further support for this hypothesis is available by utilizing 9-km WRF-1 hourly cumulative rainfall. By bracketing the rainfall accumulations between 0900 UTC 17 September 2011 and 0900 UTC 18 September 2011 we can see that WRF-1 forecasts a maximum 24-hr rain event with the entire PRE in which accumulated rainfall for Misawa increases to 100–120 mm (Figure 19).

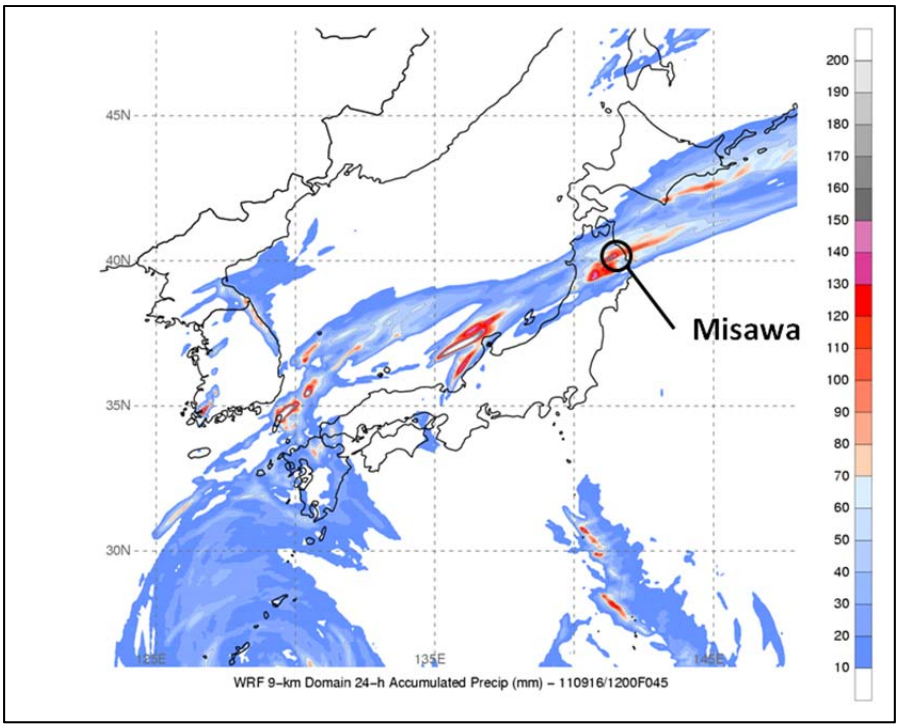


Figure 19. WRF-1 (9-km) forecast of accumulated rainfall (mm) for 0900 UTC 17 September 2011 through 0900 UTC 18 September 2011(After http://www.met.nps.edu/~hmarcham/roke/)

Given the constraints of the autonomously recorded data combined with the accumulated radar rainfall (Figure 18) and the WRF simulation accumulated rainfall (Figure 19) we conclude that the rain event that occurred over Misawa AB between 17–19 September 2011 meets the strict 100 mm 24 $h^{-1}$ criterion and therefore does qualify as a PRE.

In comparison to the PRE, the cumulative storm-related rainfall (Table 5) was 127 mm (5.00 in.), with a maximum 24-h storm rain event of 82 mm (3.23 in.). Both events occurred separately over a 96-h period (Figure 17) with very similar intensity rates during the peak maxima.

Analysis of the storm track (Figure 11) indicates that the PRE was approximately 1900 km northeast from the TC. This is notable due to the fact that during the PRE, Roke was only at TS strength. However, the impacts on rainfall at Misawa AB during the PRE were nearly identical in quantity and intensity to the impacts related to direct storm rainfall which occurred during Roke's CPA. At this time, Roke was again at TS strength but displaced only about 190 km east of Misawa AB.

### 2. PRE Characteristics

Recall the first necessary ingredient for PRE development is the existence of a longwave, upper-level trough that is favorable for frontogenesis (Cote, 2007). Between 14–17 September 2011, an eastward moving trough was evident over eastern Asia (Figure 20).

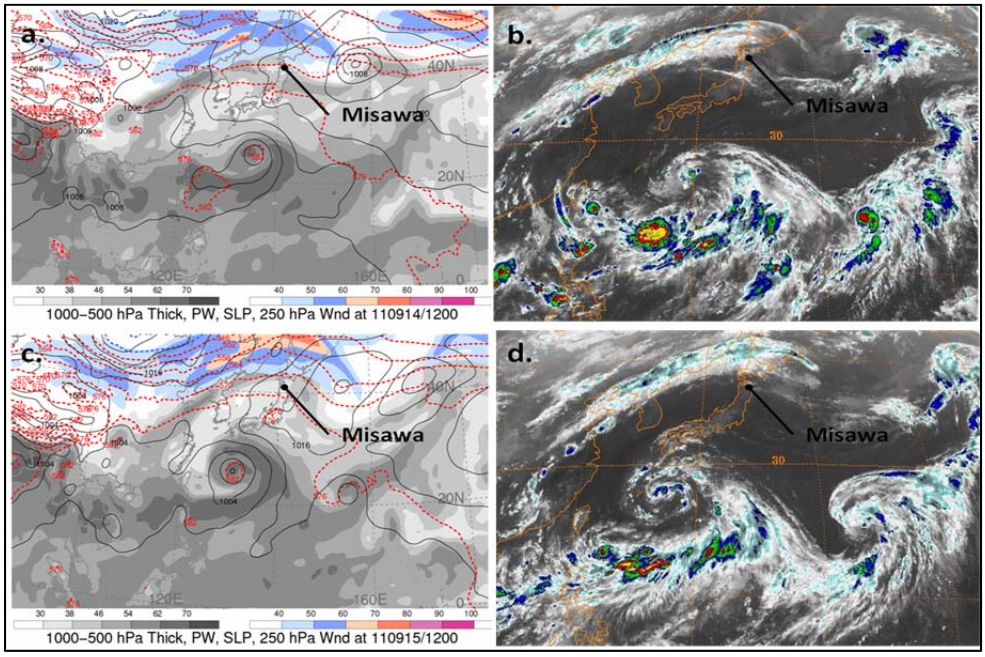


Figure 20. Analyzed GFS fields of 1000–500 hPA thickness (dashed lines in dam), precipitable water (shaded in mm), sea-level pressure (solid black line in hPA), 250 hPa wind speed (m $s^{-1}$, shaded according to color bar) for (a) 1200 UTC 14 September 2011, (c) 1200 UTC 15 September 2011 (From http://www.atmos.albany.edu/student/heathera/slp_thick/wpac/7_to_22_sep.html), color enhanced METSAT-2 full disk IR for (b) 1131 UTC 14 September 2011, (d) 1131 UTC 15 September 2011 (After http://www.ncdc.noaa.gov/)

While TS Roke was near Okinawa, the poleward moisture transport was initially blocked due to the presence of the subtropical ridge (Figures 20a–d). This feature is similar to the blocking of moisture over North America as defined by Bosart et al. 2012 in their study of PRE events associated with Atlantic TCs (Figure 1).

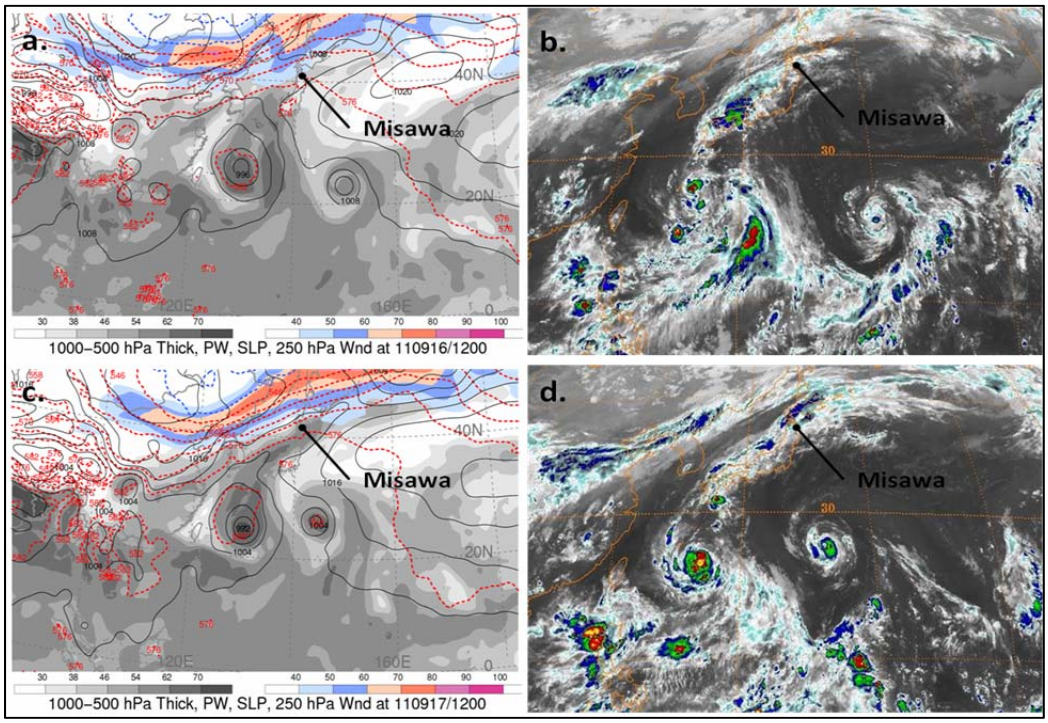


Figure 21. Analyzed GFS fields of 1000–500 hPA thickness (dashed lines in dam), precipitable water (shaded in mm), sea-level pressure (solid black line in hPA), 250 hPa wind speed (m $s^{-1}$, shaded according to color bar) for (a) 1200 UTC 16 September 2011, (c) 1200 UTC 17 September 2011 (From http://www.atmos.albany.edu/student/heathera/slp_thick/wpac/7_to_22_sep.html), color enhanced METSAT-2 full disk IR for (b) 1131 UTC 16 September 2011, (d) 1131 UTC 17 September 2011 (After http://www.ncdc.noaa.gov/)

Between 1200 UTC 15 September 2011 (Figures 20c,d) and 1200 UTC 16 September 2011 (Figures 21a,b), the subtropical ridge migrated eastward as the upper-level tropospheric trough approached from the west. Under the influence of the trough, the moisture transport from Roke was redirected poleward, and over the Japan archipelago. The removal of the subtropical ridge resulted in the arrival at Misawa of the second necessary ingredient for PRE development (Galarneau et al. 2010) near Misawa. At 1200 UTC 17 September 2011 (Figures 21c,d), when the PRE was impacting Misawa,

the moisture transport from Roke was well established as Roke was performing the cyclone loop east of Kadena AB, Okinawa.

The WRF-1 simulation on the 9-km grid (Figure 22) is examined to provide greater detail than is available with the coarse GFS analyses (Figure 21).

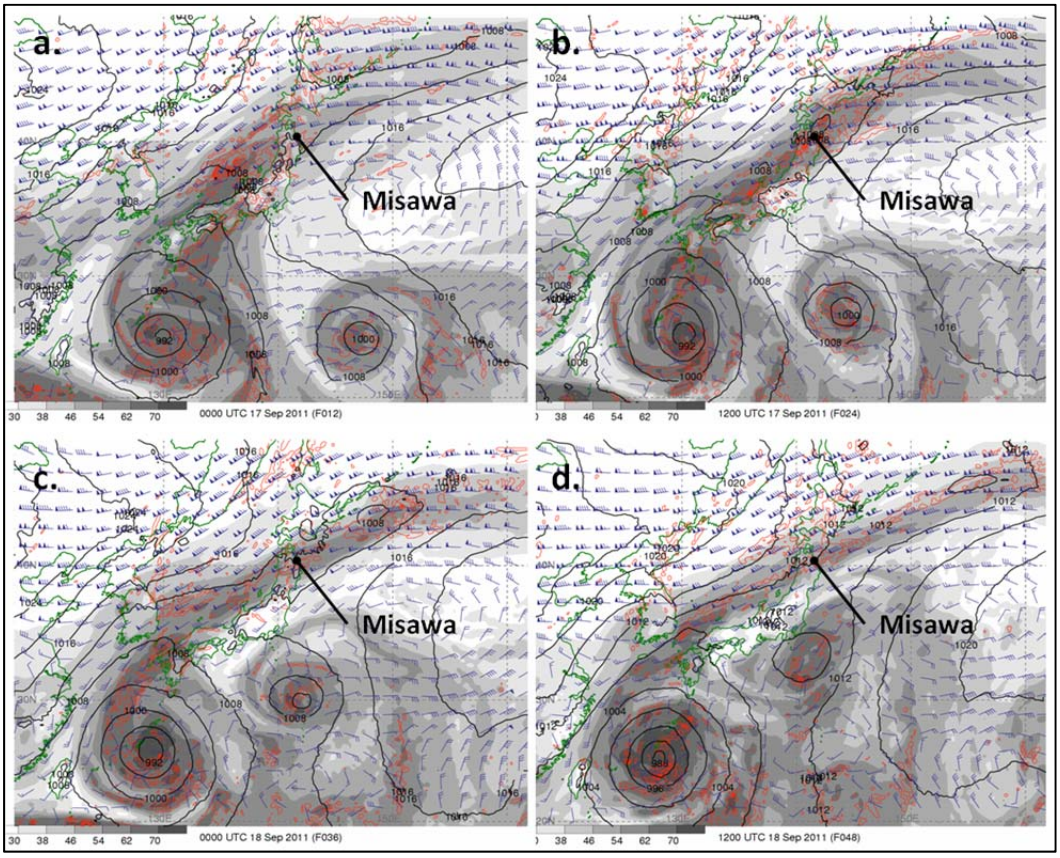


Figure 22. WRF-1 (9-km) forecast of 200 hPa wind (barbs, kt), 800–400 hPa layer-averaged ascent (red contours every 2 m $s^{-1}$, starting at 0.5 m $s^{-1}$), SLP (black contours every 4 hPa), total precipitable water (shaded in mm according to gray scale) for (a) 0000 UTC 17 September 2011, (b) 1200 UTC 17 September 2011, (c) 0000 UTC 18 September 2011, (d) 1200 UTC 18 September 2011 (After http://www.met.nps.edu/~hmarcham/roke/)

In the WRF-1 simulation, PW values increase to between 46-54 mm by 0000 UTC 17 September 2011 (Figure 22a). The WRF-1 forecast identifies the transport of PW amounts greater than 50 mm over Misawa by 1200 UTC 17 September 2011, which continues through 1200 UTC 18 September 2011 (Figures 22b–d). These PW values coincide with the maximum PRE 24-h rainfall that occurred before 0000 UTC 18

September 2011 (Table 5). Furthermore, the upper-level outflow from Roke, during this same time period, became oriented toward the mid-latitude upper-level trough (Figure 22). It should be noted here that a dry slot exists between Roke moisture and TS Sonca moisture throughout the PRE at Misawa (Figures 22a–d).

Based on the 27-km WRF-1 simulation, the region over Misawa AB was directly equatorward of the upper-level jet-entrance region during the Misawa PRE event on 17–18 September 2011 (Figure 23). Recall that development of an upper-level jet structure is consistent with forcing of the third ingredient of PRE development, which is enhanced QG forced vertical motion associated with a jet-entrance region ageostrophic circulation (Bosart et al. 2012).

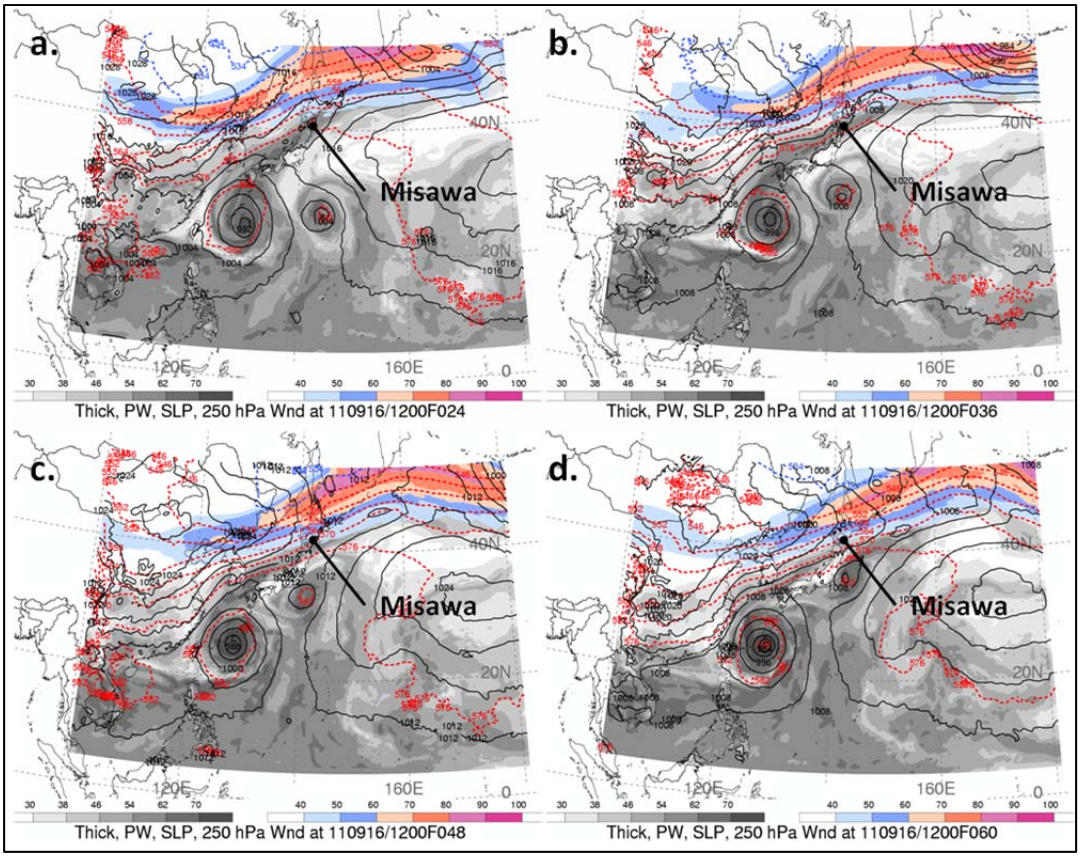


Figure 23. WRF-1 (27-km) forecast of 250 hPa wind speed (m $s^{-1}$, shaded according to color bar), 1000–500 hPa thickness (dashed contours every 6 dam), SLP (solid contours every 4 hPa), total precipitable water (mm, shaded according to gray scale) for (a) 1200 UTC 17 September 2011, (b) 0000 UTC 18 September 2011. (c) 1200 UTC 18 September 2011, (d) 0000 UTC 19 September 2011 (After http://www.met.nps.edu/~hmarcham/roke/)

The upper-level jet continues to be present poleward of Misawa during the first 12 h of the PRE between 1200 UTC 17 September 2011 (Figure 23a) and 0000 UTC 18 September 2011 (Figure 23b). Over the next 12 h, during the most intense rainfall (Figure 18b), the jet-entrance region locks in place and reaches its maximum intensity (Figure 23c) poleward of Misawa. The upper-level jet begins to migrate northeast of Japan by 0000 UTC 19 September 2011 (Figure 23d), which is the end of the PRE impact at Misawa AB.

To examine the possibility of QG-forcing of vertical motion as a contribution to enhanced vertical motion during the Misawa PRE, Q-vector convergence was plotted on temperature and wind fields for the WRF forecast model (Figure 24).

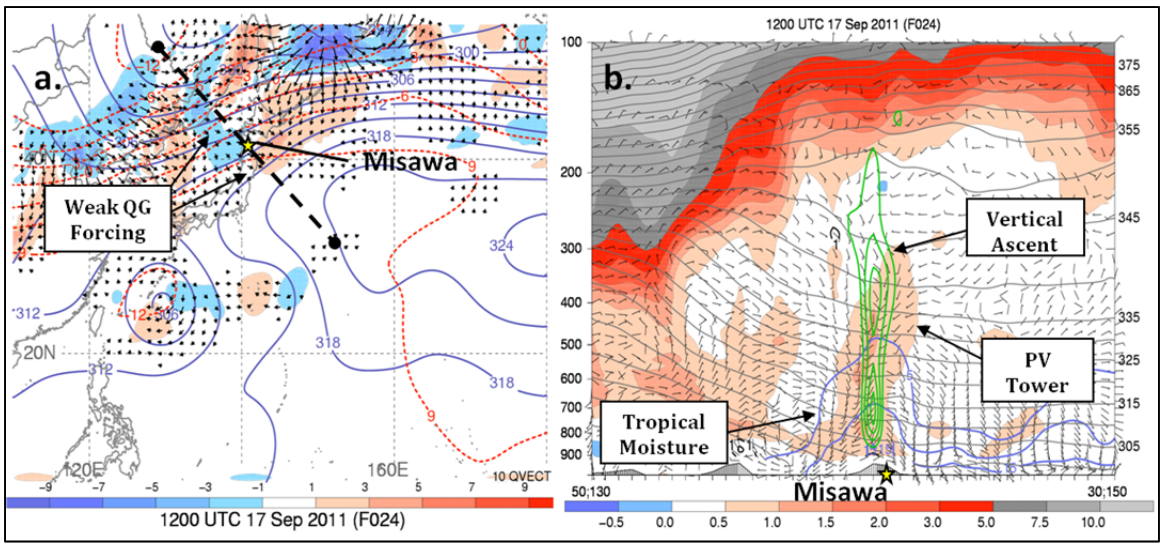


Figure 24. (a) WRF-1 (27-km) forecast of 700 hPa geopotential height (solid blue, dam), temperature (dashed red, °C), Q vector (arrows, plotted for values greater than 5 x $10^{-7}$ Pa $m^{-1}$ $s^{-1}$ only), and Term A of the Q-vector form of the QG Omega equation (shaded $10^{-12}$ Pa $m^{-2}$ $s^{-1}$) for 1200 UTC 17 September 2011, and (b) WRF-1 (27-km) jet-entrance cross sections of PV (shaded, PVU), potential temperature (gray contours, every 5 K), ageostrophic wind (barbs, kt), frontogenesis (black contours, every 1 °C 100 $km^{-1}$ 3 $h^{-1}$, mixing ratio (blue contours, every 5 g $kg^{-1}$), ascent (green contours, every 1 m $s^{-1}$) for 1200 UTC 17 September 2011 (After http://www.met.nps.edu/~hmarcham/roke/)

At 1200 UTC 17 September 2011 (Figures 24a,b), which is the start of the maximum PRE rainfall at Misawa (Figure 17), Q-vector convergence existed directly over northern Honshu while Q-vector divergence occurs just northeast over the Sea of Japan (Figure

24a). This indication of QG-forcing coincides with the upper-level jet-entrance region located poleward of Misawa at this time (Figure 23a), which suggests the potential presence of a jet-entrance region ageostrophic circulation. At this time, the jet core is located to the northwest of Misawa between 500–300 hPA (Figure 25) in the region of maximum vertical slope of the upper-level potential vorticity (PV).

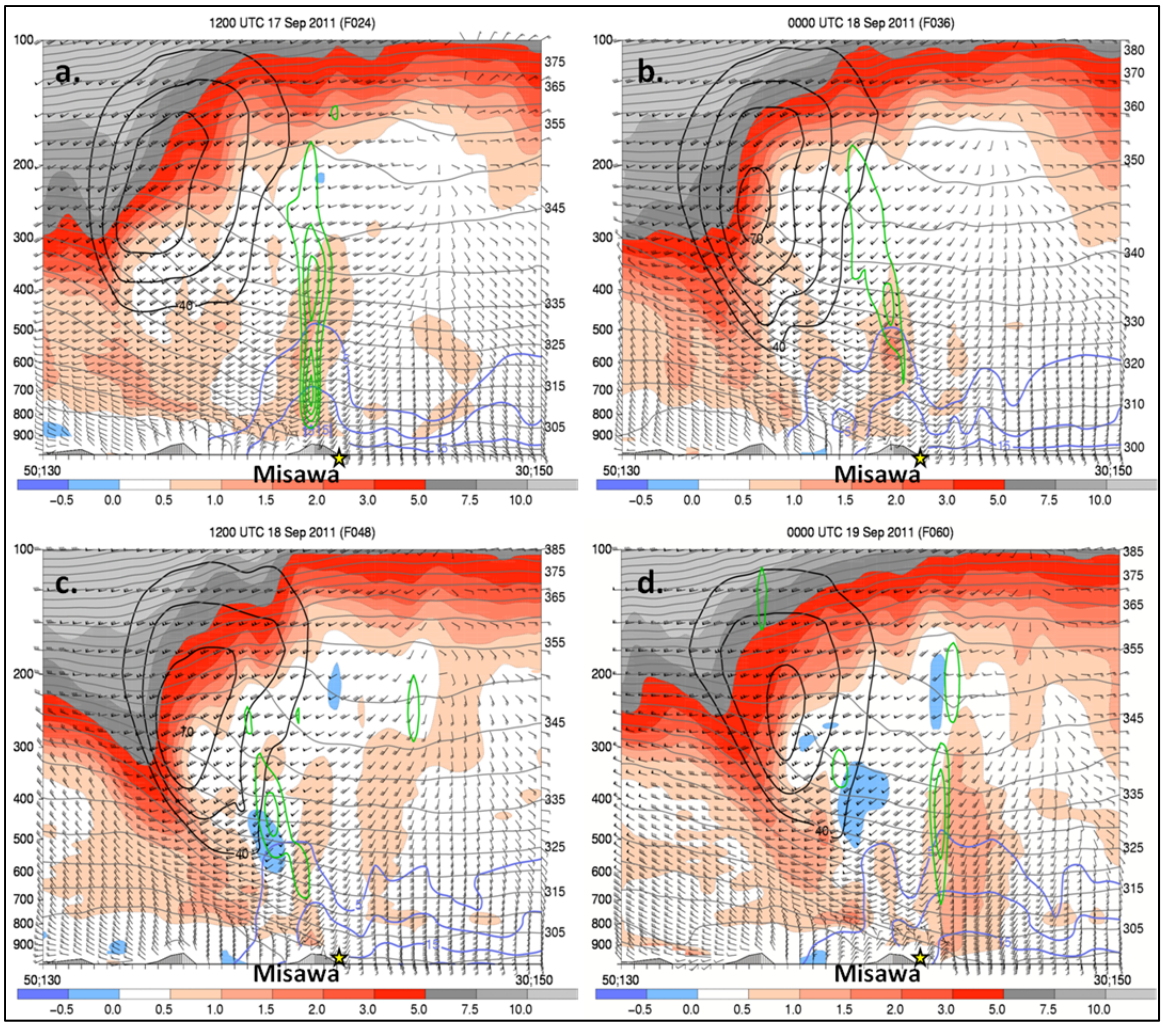


Figure 25. WRF-1 (27-km) jet-entrance cross section forecast of PV (shaded, PVU), potential temperature (gray contours, every 5 K), full wind (barbs, kt), jet core wind speed (black contours, every 10 m $s^{-1}$, starting at 40 m $s^{-1}$, mixing ratio (blue contours, every 5 g $kg^{-1}$), ascent (green contours, every 1 m $s^{-1}$) for (a) 1200 UTC 17 September 2011, (b) 0000 UTC 18 September 2011, (c) 1200 UTC 18 September 2011, (d) 0000 UTC 19 September 2011 (After http://www.met.nps.edu/~hmarcham/roke/)

This steep PV gradient is a direct result of the underlying developing baroclinic condition near Misawa. During this period southerly ageostrophic winds exist to 200 hPA, directly over Misawa (Figure 24b). These winds coincides with poleward-oriented transport into the region near Misawa. The moisture plume extends from Roke to the northeast and over Misawa (Figure 22b). At the upper-levels, the southerly ageostrophic winds over Misawa turn from the southeast and cross the upper-level jet core to the north of Misawa (Figure 24b). The combination of the rising motion over Misawa (Figure 24b) and southerly ageostrophic flow over Misawa with the across jet ageostrophic winds at upper-levels represent the rising branch and the upper-level across jet branch of the ageostrophic circulation at the jet-entrance region. Beneath the jet and to the northwest of Misawa there is some enhancement of the low-level baroclinic zone (Figure 24b), but frontogenesis in the region is small at this time. The combination of weak QG forcing (Figure 24a) and no frontogenesis (Figure 24b) suggests that at the onset of the PRE the predominant mechanism was large-scale lifting of the moisture plume as it arrived in the region of Misawa.

Over Misawa, the convective condition of the PRE also define a PV-tower that extends up to 300 hPA (Figure 24b). Furthermore, the strong ascent exists up to 200 hPA (Figure 24b), and the rising motion bisects the highest concentrations of moisture residing directly over Misawa.

By 0000 UTC 18 September 2011 (Figures 26a,b), which is the period of most intense rainfall over Misawa (Figure 17), weak QG forcing still exists over the region as defined by Q-vectors that point across isentropes toward warm air over Misawa (Figure 26a).

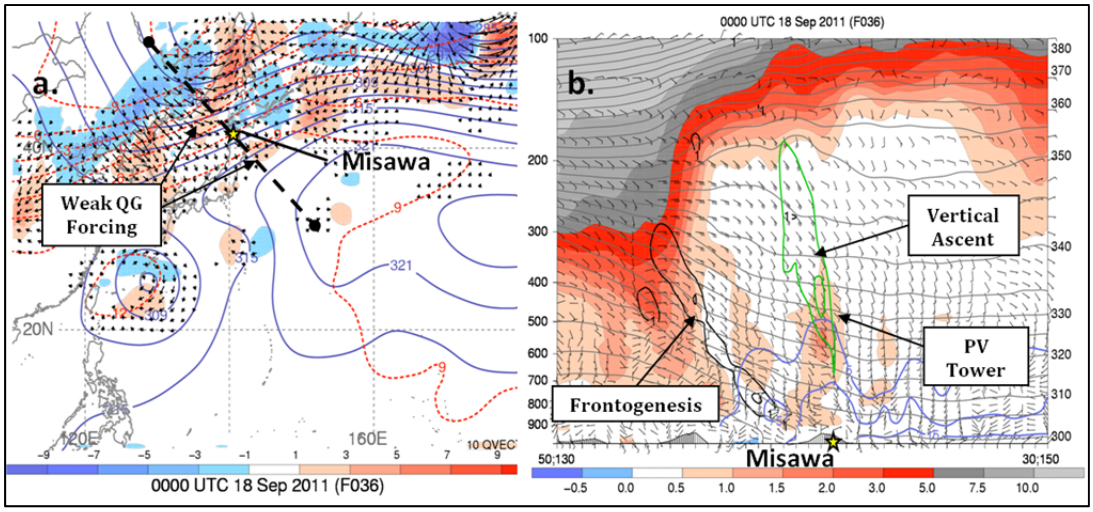


Figure 26. (a) WRF-1 (27-km) forecast of 700 hPa geopotential height (solid blue, dam), temperature (dashed red, °C), Q vector (arrows, plotted for values greater than 5 x $10^{-7}$ Pa $m^{-1}$ $s^{-1}$ only), and Term A of the Q-vector form of the QG Omega equation (shaded $10^{-12}$ Pa $m^{-2}$ $s^{-1}$) for 0000 UTC 18 September 2011, and (b) WRF-1 (27-km) jet-entrance cross sections of PV (shaded, PVU), potential temperature (gray contours, every 5 K), ageostrophic wind (barbs, kt), frontogenesis (black contours, every 1 °C 100 $km^{-1}$ 3 $h^{-1}$, mixing ratio (blue contours, every 5 g $kg^{-1}$), ascent (green contours, every 1 m $s^{-1}$) for 0000 UTC 18 September 2011 (After http://www.met.nps.edu/~hmarcham/roke/)

This is a clear indication of horizontal frontogenesis in the presence of a developing baroclinic zone (Martin 2006), which is identified by the cross section across the jet (Figure 26b). At this time, the jet core is still located to the northwest of Misawa and the slope of the upper-level PV gradient has steepened over Misawa and now extends between 150–500 hPA (Figure 25b).

The jet streak northwest of Misawa has intensified (Figure 23b) and the maximum jet core wind speed increased to 70 m $s^{-1}$ (Figure 25b). The path of southerly and rising ageostrophic winds over Misawa increased in magnitude (Figure 26b). Furthermore the ageostrophic winds continue to cross the upper-level jet core over Misawa (Figure 26b). Therefore the two branches of the ageostrophic circulation at the jet-entrance region are still present and intensifying. At this time frontogenesis beneath the jet extends southeastward and downward along the sloping baroclinic zone toward the northwest of Misawa (Figure 26b).

Over Misawa, the PRE is still defined by a PV-tower, however now it only extends to 400 hPA (Figure 26b). The PRE is still located in a region of strong ascent over Misawa, however the ascent axis has begun to slope toward the jet core (Figure 25b). Furthermore Q-vector convergence remains low over Misawa (Figure 26a) and low-level frontogenesis is not present over Misawa (Figure 26b) during this time. Therefore the continuation of the PRE is predominantly due to high available moisture content in a region of developing instability that only requires slight lifting to create and maintain an enhanced rain fall event.

At 1200 UTC 18 September 2011 (Figures 27a,b), rainfall over Misawa began to decrease intensity (Figure 18d).

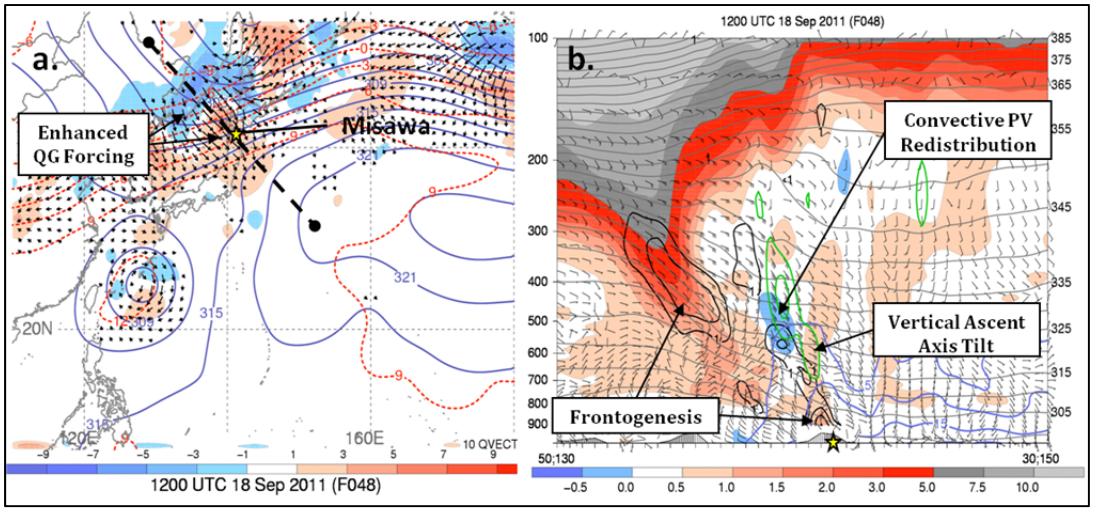


Figure 27. (a) WRF-1 (27-km) forecast of 700 hPa geopotential height (solid blue, dam), temperature (dashed red, °C), Q vector (arrows, plotted for values greater than 5 x $10^{-7}$ Pa $m^{-1}$ $s^{-1}$ only), and Term A of the Q-vector form of the QG Omega equation (shaded $10^{-12}$ Pa $m^{-2}$ $s^{-1}$) for 1200 UTC 18 September 2011, and (b) WRF-1 (27-km) jet-entrance cross sections of PV (shaded, PVU), potential temperature (gray contours, every 5 K), ageostrophic wind (barbs, kt), frontogenesis (black contours, every 1 °C 100 $km^{-1}$ 3 $h^{-1}$, mixing ratio (blue contours, every 5 g $kg^{-1}$), ascent (green contours, every 1 m $s^{-1}$) for 1200 UTC 18 September 2011 (After http://www.met.nps.edu/~hmarcham/roke/)

The QG forcing of vertical motion has increased in the region (Figure 27a) and the Q-vectors are oriented almost directly perpendicular to isentropes. At this time, the jet core remains northwest of Misawa with the PV gradient has reaching its steepest slope

now between 200–500 hPA (Figure 25c). The jet streak northwest of Misawa has consolidated (Figure 23c) and the maximum jet core wind speed of 70 m $s^{-1}$ remains unchanged (Figure 25c).

Over Misawa, the PV-tower has decreased in intensity (Figure 27b) as the PRE rainfall over Misawa begins to decrease at 1200 UTC 18 September 2011 (Figure 17). However, the ageostrophic winds continue to increase in magnitude (Figure 27b) and frontogenesis is now present at low-levels over Misawa (Figure 27b). The southerly ageostrophic winds coincide with a region of vertical motion that corresponds to the connected region of frontogenesis that extends upward from the upper-level jet northwest of Misawa (Figure 27b). The tropopause behind the front is clearly lowering in response to the now overriding ageostrophic frontogenetic circulation (Figure 27b). Beneath the jet northeast of Misawa, convective PV redistribution occur along the frontal boundary (Figure 25c). Although the tropical moisture plume is still present over Misawa, the vertical ascent axis has tilted more to the northwest over the frontal boundary, which suggest that the rainfall during this period may be due to the low-level frontogenesis (Figure 27b).

By 0000 UTC 19 September 2011 (Figures 28a,b), the PRE rainfall over Misawa has ended (Figure 17). The QG forcing in the region appears to have migrated to the northeast (Figure 28b) as the jet-streak migrates downstream along the eastward moving upper-level trough. An enhanced region of QG forcing of vertical motion appears west of Misawa (Figure 28a). The jet core wind speed maximum has decreased to 60 m $s^{-1}$ (Figure 25d). Beneath the jet, upper-level frontogenesis along the frontal boundary is still present (Figure 28b).

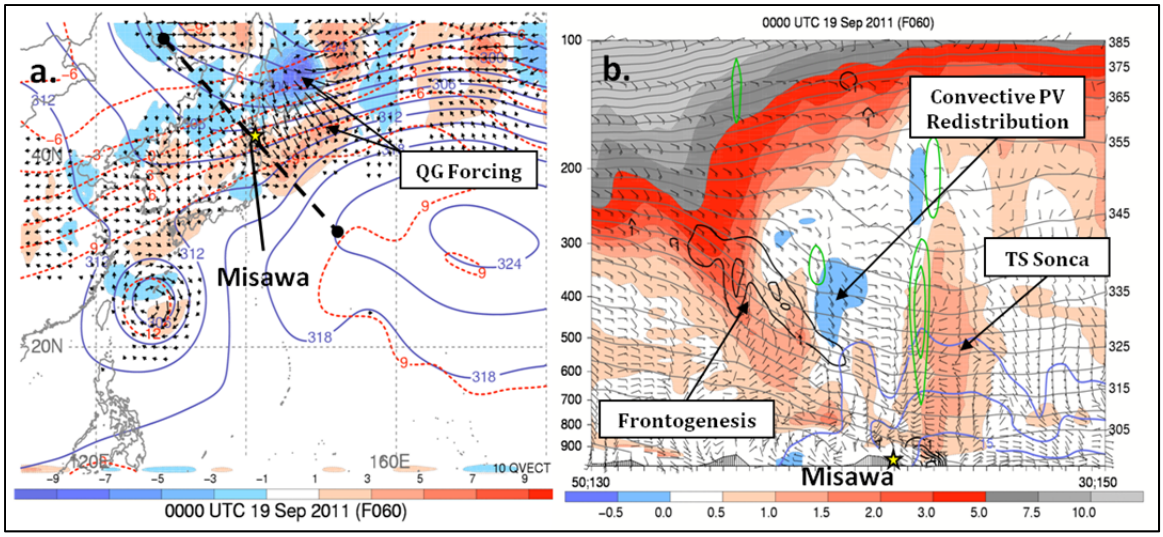


Figure 28. (a) WRF-1 (27-km) forecast of 700 hPa geopotential height (solid blue, dam), temperature (dashed red, °C), Q vector (arrows, plotted for values greater than 5 x $10^{-7}$ Pa $m^{-1}$ $s^{-1}$ only), and Term A of the Q-vector form of the QG Omega equation (shaded $10^{-12}$ Pa $m^{-2}$ $s^{-1}$) for 0000 UTC 19 September 2011, and (b) WRF-1 (27-km) jet-entrance cross sections of PV (shaded, PVU), potential temperature (gray contours, every 5 K), ageostrophic wind (barbs, kt), frontogenesis (black contours, every 1 °C 100 $km^{-1}$ 3 $h^{-1}$, mixing ratio (blue contours, every 5 g $kg^{-1}$), ascent (green contours, every 1 m $s^{-1}$) for 0000 UTC 19 September 2011 (After http://www.met.nps.edu/~hmarcham/roke/)

Over Misawa, the lower-level frontogenesis has decreased and the highest moisture concentrations are seen west of Misawa (Figure 28b). Southeast of Misawa a strong PV-tower and region of enhanced vertical ascent is present, however this feature represents the presence of TS Sonca approaching Misawa from the southeast (Figure 28b) and is too far away to impact Misawa directly (Figure 22d).

The analysis of low and upper-level features associated with the PRE at Misawa varies somewhat from the Bosart et al. (2012) proposal of ageostrophic circulation as the primary contribution to an increase in PRE rainfall due to enhancement of vertical motion of already saturated air. In the case of Roke the PRE began prior to the maximum QG forcing and frontogenesis. However, these forcing mechanisms were responsible for maintaining the PRE beyond 24-hr. It further highlights the spatial details and the temporal forecasting requirements to accurately predict these events.

## B. MISAWA STORM EVENT

In contrast to the PRE dynamics, the storm-induced rainfall over Misawa was due to available moisture and dynamical processes associated with the tropical cyclone itself when Roke passed its CPA to Misawa at 1500 UTC 21 September 2011. There is a region of greatly enhanced QG forcing associated with a tropical cyclone (Figure 29a).

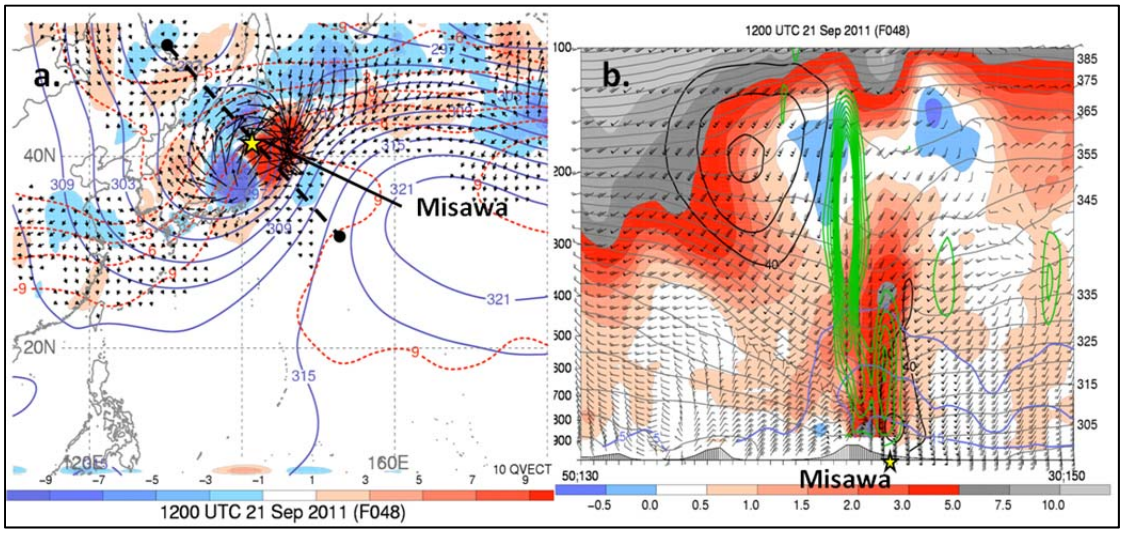


Figure 29. (a) WRF-2 (27-km) forecast of 700 hPa geopotential height (solid blue, dam), temperature (dashed red, °C), Q vector (arrows, plotted for values greater than 5 x $10^{-7}$ Pa $m^{-1}$ $s^{-1}$ only), and Term A of the Q-vector form of the QG Omega equation (shaded according to the colorbar, $10^{-12}$ Pa $m^{-2}$ $s^{-1}$) for 1200 UTC 21 September 2011, and (b) WRF-2 (27-km) jet-entrance region cross section of PV (shaded, PVU), potential temperature (gray contours, every 5 K), full wind (barbs, kt), wind speed (black contours, every 10 m $s^{-1}$, starting at 40 m $s^{-1}$, mixing ratio (blue contours, every 5 g $kg^{-1}$), ascent (green contours, every 1 m $s^{-1}$) for 1200 UTC 21 September 2011 (After http://www.met.nps.edu/~hmarcham/roke/)

The QG forcing of upward motion due to Roke passing its CPA to Misawa (Figure 29a) is much stronger than the forcing associated with the PRE. There is Q-vector convergence ahead, to the northeast along the track of Roke, and Q-vector divergence behind (Figure 29a). This is a common feature associated with a TC that is undergoing extra-tropical transition (ET).

The vertical cross section across Misawa and Roke (Figure 29b) identifies the enhanced region of ascent that extends from low-levels to 150 hPA which is in contrast to the tilting, and less vertical, ascent along the frontal boundary at the time of the PRE

(Figure 27b). The PV-tower associated with the TC is greater in magnitude and extends farther into the troposphere with a well defined region of convective PV redistribution throughout the troposphere (Figure 29b).

The rain event associated with the passing of Roke over Misawa AB between 20-21 September 2011 (Figure 17) at CPA coincides with the ET of Roke as it crosses the upper-level trough axis. An along track cross section of ageostrophic winds and ascent helps confirm the ascending air ahead of Roke as it underwent ET (Figures 30).

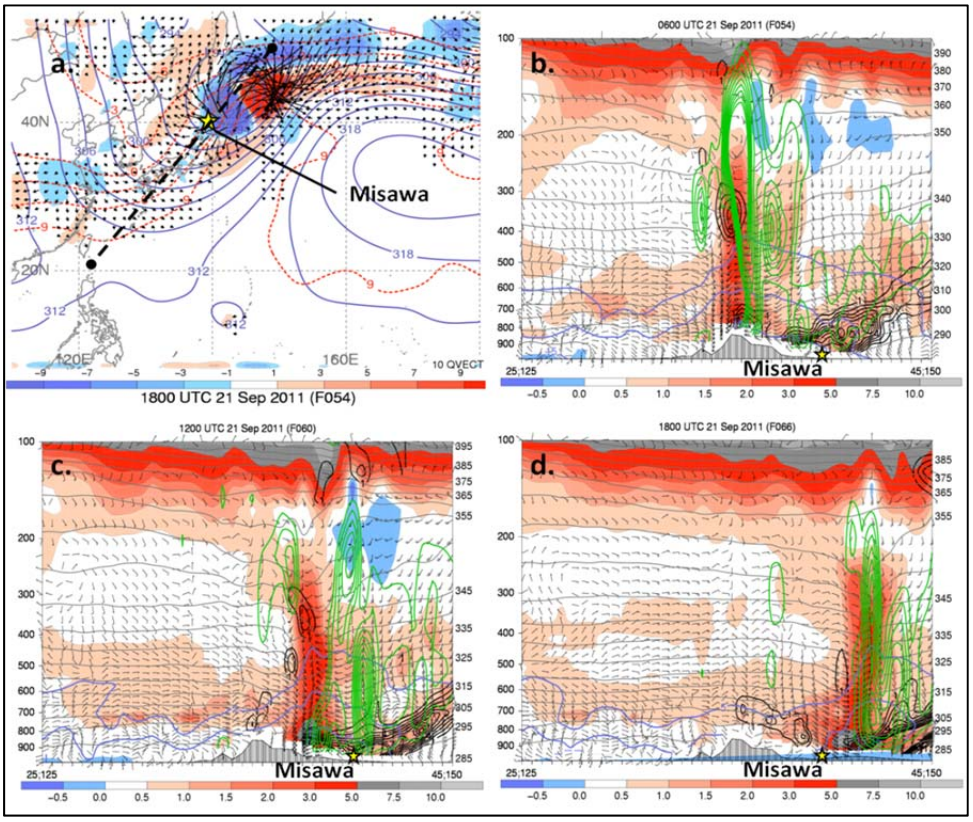


Figure 30. (a) WRF-2 (27-km) forecast of 700 hPa geopotential height (solid blue, dam), temperature (dashed red, °C), Q vector (arrows, plotted for values greater than 5 x $10^{-7}$ Pa $m^{-1}$ $s^{-1}$ only), and Term A of the Q-vector form of the QG Omega equation (shaded according to the colorbar, $10^{-12}$ Pa $m^{-2}$ $s^{-1}$) for 1800 UTC 21 September 2011, and WRF-2 (27-km) along track cross-section of PV (shaded, PVU), potential temperature (gray contours, every 5 K), ageostrophic wind (barbs, kt), frontogenesis (black contours, every 1 °C 100 $km^{-1}$ 3 $h^{-1}$, mixing ratio (blue contours, every 5 g $kg^{-1}$), ascent (green contours, every 1 m $s^{-1}$) for (b) 0600 UTC 21 September 2011, (c) 1200 UTC 21 September 2011, and (d) 1800 UTC 21 September 2011. (After http://www.met.nps.edu/~hmarcham/roke/)

The rain during this period is due to strong frontogenesis along a cyclone-induced warm frontal boundary ahead of Roke at 0600 UTC 21 September 2011 (Figure 30b). As Roke passes over Misawa, the rainfall is attributed to the deep convection and strong ascent of tropical moisture associated with the TC dynamics itself represented by a strong PV-tower (Figure 30b) at 1200 UTC September 2011. The rain continues over Misawa due to weak low-level frotogenesis along a cold frontal boundary behind Roke at 1800 UTC September 2011 (Figure 30c). This time series of shifting dynamical frontogenetic processes helps support the conclusion that Roke completed ET over Misawa, as represented by stronger warm frontogenesis ahead and weak cold frontogenesis behind Roke during ET. (Harr and Elsberry, 2000)

## C. NAGASAKI SIGNIFICANT RAIN EVENT

Nagasaki began experiencing heavy rainfall at 0000 UTC 18 September 2011 (Figure 31), however the heavy rain only lasted for 12 h until 1200 UTC 18 September 2011.

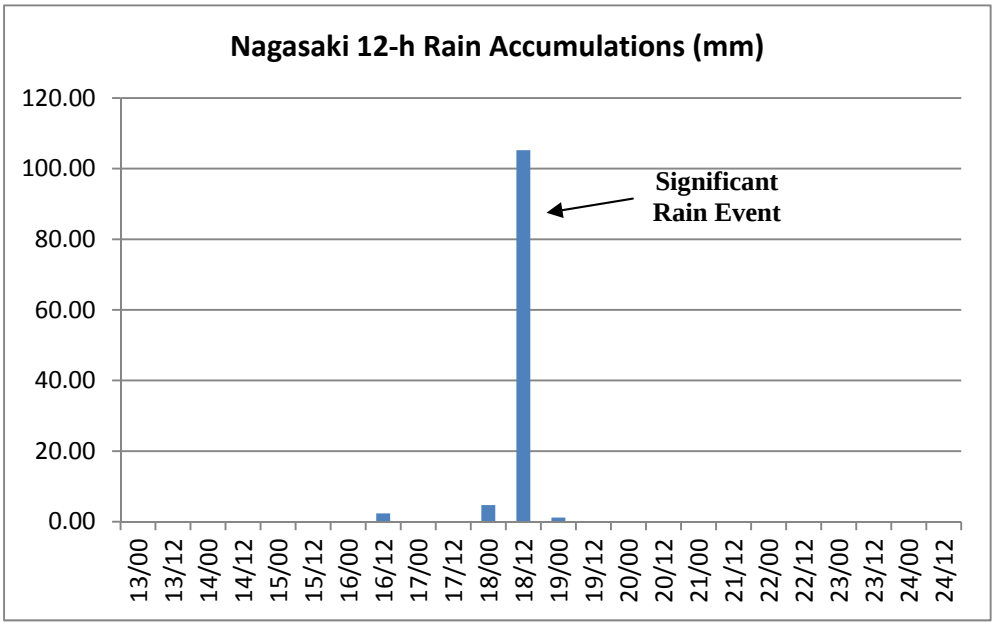


Figure 31. Nagasaki rainfall histogram with 12 h bin size for 0000 UTC 13 September 2011 through 1200 UTC 24 September 2011 collected from NCDC

The NCDC data indicate that the event lasted 36 h (1.5 days). The cumulative rainfall for this event was 112 mm (4.41 in.) with 110 mm (4.33 in.) falling in a 12 h period with 1 mm (0.04 in.) falling on either side of that 12 h period.

The rainfall event at Nagasaki does meet the strict threshold of 100 mm 24 $h^{-1}$ set by Cote (2007) to be considered for classification as a PRE however, diagnosis of the WRF simulation for this event (Figure 32) do not support classification of this event as a PRE.

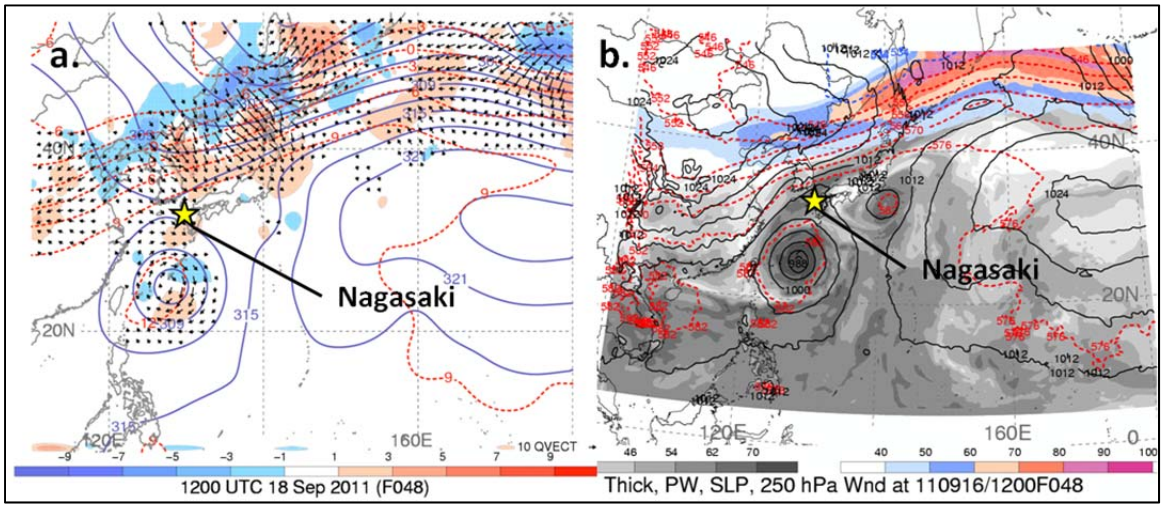


Figure 32. (a) WRF-1 (27-km) forecast of 700 hPa geopotential height (solid blue, dam), temperature (dashed red, °C), Q vector (arrows, plotted for values greater than 5 x $10^{-7}$ Pa $m^{-1}$ $s^{-1}$ only), and Term A of the Q-vector form of the QG Omega equation (shaded according to the colorbar, $10^{-12}$ Pa $m^{-2}$ $s^{-1}$) for 1200 UTC 18 September 2011, and (b) WRF-1 (27-km) forecast of 250 hPa wind speed (m $s^{-1}$, shaded according to color bar), 1000–500 hPa thickness (dashed contours every 6 dam), SLP (solid contours every 4 hPa), total precipitable water (mm, shaded according to gray scale) for 1200 UTC 18 September 2011 (After http://www.met.nps.edu/~/hmarcham/roke/)

At 1200 UTC 18 September 2011, during the Nagasaki significant rain event, QG forcing in the area is weak (Figure 32a). Although the high PW moisture plume (Figure 32b) does extend over Nagasaki from Roke it is unclear whether all the moisture is coming from Roke or if some of the moisture is actually emanating from TS Sonca which is due west of Nagasaki during the event. Although Nagasaki is located in a region of a persistent upper-level longwave trough (Figure 32a), the region directly over Nagasaki

does not appear to be favorable for mid-level frontogenesis as the developed baroclinic zone is located more poleward of Nagasaki and oriented northeastward over the Sea of Japan and Misawa (Figure 32a). Finally, the upper-level jet at the time of the event appears to be displaced too far poleward for the area over Nagasaki to be influenced by an associated jet-entrance region ageostrophic circulation (Figure 32b).

To confirm the hypothesis that the significant Nagasaki rain event does not meet the classification of a PRE, radar imagery for the event was compared with WRF-1 accumulated precipitation forecasts (Figure 33).

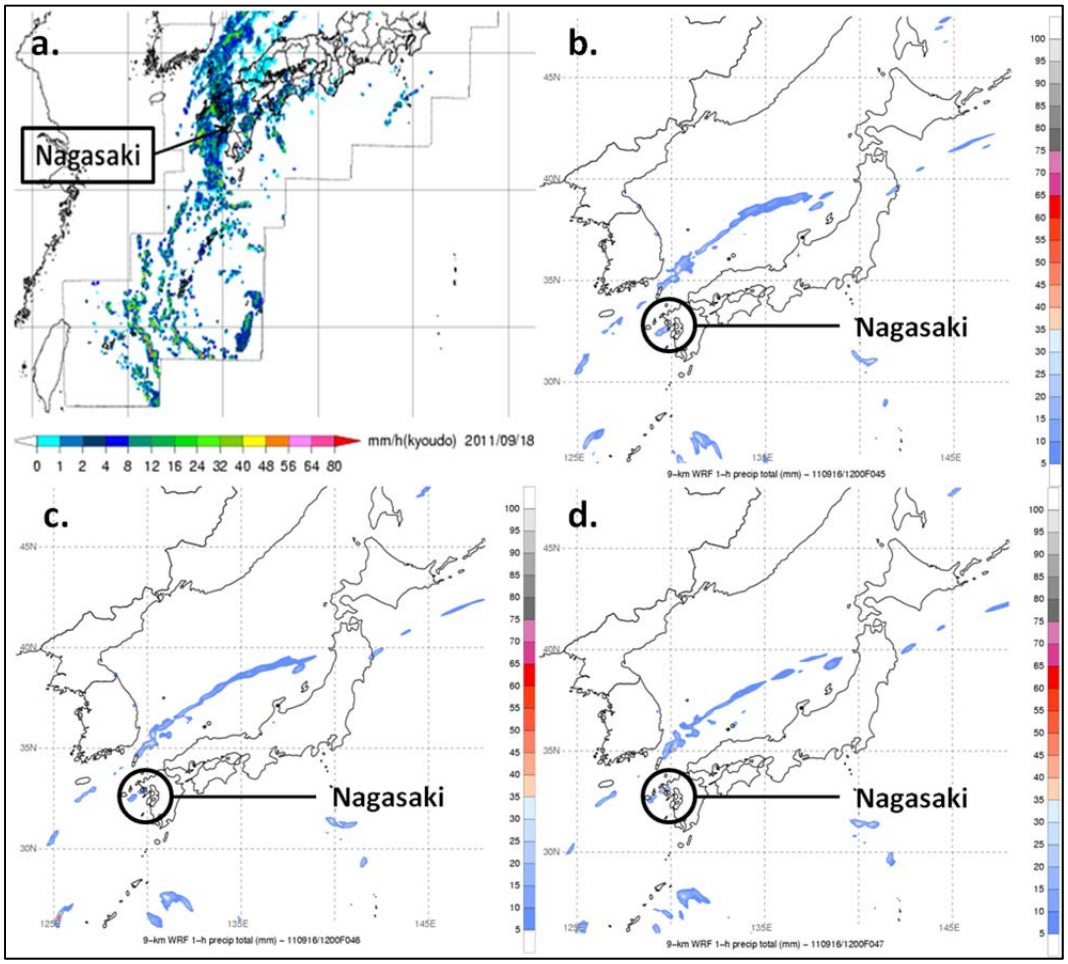


Figure 33. (a) Radar derived hourly rain rates (mm $h^{-1}$) for 1200 UTC 18 September 2011, and WRF-1 (9-km) forecast of 1 h accumulated rainfall (mm) for (b) 0900 UTC 18 September 2011, (c) 1000 UTC 18 September 2011, (d) 1100 UTC 18 September 2011 (After http://www.met.nps.edu/~hmarcham/roke/)

Radar imagery shows that a band of convective activity existed northward from Roke due north at the time of the significant Nagasaki rain event at 1200 UTC 18 September 2011 (Figure 33). This is in contrast to the northeastward oriented line of convective activity draped across the frontal boundary that existed over the Sea of Japan and Misawa during the Misawa PRE (Figure 18). Forecasted rainfall accumulations using WRF-1 were analyzed for the 12 h period covered by the single Nagasaki rain accumulations peak recorded by NCDC for this time period (Figure 31). The only WRF-1 forecast rain accumulations over Nagasaki that were registered occurred between 0900 UTC through 1100 UTC 18 September 2011 (Figures 33b–d). At 1000 UTC an isolated rainfall accumulation of greater than 50 mm occurred in a 1 h period (Figure 33d) preceded by two 1 h periods of light rainfall 20-30 mm each (Figures 33b,c). This total 3 h period of isolated rainfall helps confirm that the significant rain event at Nagasaki was not a PRE, but instead an isolated incident of convective activity in a region of highly saturated air.

The recorded rainfall at Nagasaki occurred predominantly in one 12 h period between 0000 UTC through 1200 UTC 18 September 2011 (Figure 31) and was almost equal in magnitude to the two-day (124 mm) PRE that occurred over Misawa AB (Table 5). This makes the rainfall intensity at Nagasaki twice as intense (110 mm 12 $h^{-1}$) as the peak 24 h rainfall period experienced at Misawa (100-120 mm 24 $h^{-1}$). The significant rain event at Nagasaki was worth mentioning in this thesis due to its proximity to the 2nd largest U.S. Navy Fleet concentration within USFJ at Fleet Activities Sasebo.

# V. CONCLUSION AND RECOMMENDATION

Land-falling tropical cyclones are often connected with one or more destructive forces including high winds greater than 50 kt, storm surges, enhanced swell activity, and heavy rainfall. Predecessor rain events (PRE) have been linked to the tropical moisture content surrounding TCs that are displaced thousands of kilometers away and days ahead of actual TC landfall. The U.S. Navy and DoD focus primarily on the arrival of one destructive force, sustained high winds, when issuing TCCORs in connection with emergency preparedness procedures. The purpose of this thesis was to highlight the fact that heavy rainfall events, under specific conditions, are directly connected with the tropical cyclones that are significantly displaced in time and space from the rain event via transport of tropical moisture, and consideration for these events should be included in the DoD emergency preparedness procedures.

## A. MISAWA AIR BASE PRE IMPACTS

Between 17–19 September 2011 Misawa AB, Japan recorded 124 mm (4.88 in.) total rainfall containing a recorded maximum 24 h intensity of 84 mm 24 $h^{-1}$. Because of the limitations of the autonomously recorded rainfall data, WRF was utilized to show that the maximum 24 h rainfall intensity during this period was 100–120 mm 24 $h^{-1}$, which is a specific requirement for classification as a PRE (Cote 2011). Further analysis of WRF simulations for this rainfall event indicate that it had both the mid-latitude and tropical ingredients as well as the dynamic characteristics of a PRE, which include an upper-level longwave trough favorable for the development of midlevel frontogenesis (Cote 2007), an available moisture plume surrounding TC Roke with PW values greater than 50 mm (Galarneau et al. 2010), transport of tropical moisture poleward from Roke in response to a retreating subtropical ridge (Galarneau et al. 2010), QG forced ascent associated with the jet-entrance region (Bosart et al. 2012), and a developing baroclinic zone that led to enhanced frontogenesis over Misawa AB. These contributing factors combined with the fact that Roke was over 1900 km southwest and 4 days away from Misawa AB at the time, allow this rain event to be classified as a PRE.

This is of significance because the total rainfall during the Misawa PRE (124 mm) was almost identical to the 127 mm (5 in.) rainfall that occurred when Roke passed its CPA to Misawa on 21 September 2011. Misawa was only displaced 190 km east of Roke during CPA and experienced a nearly identical maximum 24 h rainfall intensity peak as it did during the PRE when Roke was 1900 km away. This bimodal rainfall distribution (Figure 17) is a common signature of along track PREs associated recurving TCs.

The 35th Fighter Wing Operations and Support Squadron (OSS) is responsible for TCCOR recommendations to the 35th Fighter Wing Commander who is the local TCCOR authority per COMNAVFORJAPANINST 3140.4A. Recall that the original forecast on 11 September 2011 called for TC Roke to pass south and west of the main island of Honshu and Misawa AB. It was not until 1800 UTC 16 September 2011 that the forecast track for TC Roke transformed from a straight runner to a recurver TC its projected swath of influence began to incorporate the main island of Honshu (Figure 34). Only 6-h later at 0000 UTC 17 September 2011, which is when the forecast track fully incorporated northern Honshu Island (and Misawa AB), the PRE had already began to impact Misawa.

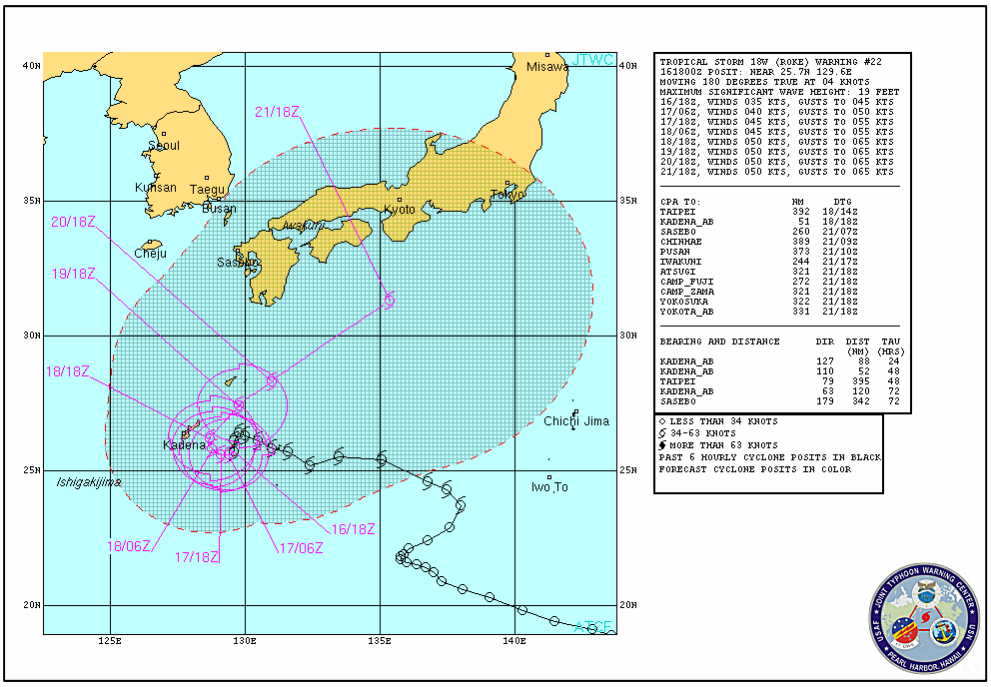


Figure 34. TS Roke warning #22 for 1800 UTC on 16 September 2011, (From JTWC)

The 35th Fighter Wing Operations never recommended that Misawa AB be placed in a heightened state of readiness with regards to TC Roke, nor should they have based on the current procedures they have available. Misawa AB stayed in a TCCOR "ALL CLEAR" readiness state throughout the duration of TC Roke and for both the PRE and storm rain events even though they experienced a predictable high impact rain event.

## B. NAGASAKI SIGNIFICANT RAIN EVENT IMPACTS

On 18 September 2011 Nagasaki, Japan recorded 112 mm (4.41 in.) total rainfall containing a recorded maximum 24 h intensity of 110 mm 12 $h^{-1}$. This makes the rainfall experienced over Nagasaki twice as intense as the maximum intensity of rain witnesses over Misawa. The significant rain event over Nagasaki occurred while being displaced in time (2 days ahead) and space (900 km) from Nagasaki. Although the rainfall intensity experienced over Nagasaki meets strict 100 mm 24 $h^{-1}$ PRE requirement, WRF simulations of this event help us to conclude that it does not meet the requirements for classification as a PRE, but instead as an isolated significant rain event. WRF simulations did confirm that the available moisture over Nagasaki was directly related to tropical moisture transport from Roke leading to potential further research into convective processes along tropical moisture transport paths that can lead to these anomalous rain events.

The NOAC, Yokosuka is responsible for TCCOR recommendations to Commander, U.S. Fleet Activities Sasebo, who is the delegated local TCCOR authority for FAS. The NOAC Yokosuka never recommended that FAS, which is located approximately 47 km northwest of Nagasaki, be placed in a heightened TCCOR. FAS remained in a TCCOR "ALL CLEAR" readiness state throughout the significant rain event due to the current TCCOR procedures available.

## C. OPNAVINST 3140.24F RECOMMENDATION

The primary reason for recommending a change to DoD emergency preparedness instructions, specifically OPNAVINST 3140.24F, is the link between tropical cyclone moisture, which is a direct byproduct of the TC, and its ability to be transported thousands of kilometers away from the TC itself. The WRF simulation helps confirm

that predicting this “invisible” moisture plume transport is possible, and that the plume itself, when intersecting regions of baroclinic instability, warrants caution due to the potential for PRE activity. Because excessive rainfall is a potentially destructive and deadly force associated with TCs, the TCCOR process should incorporate, at a minimum, the definition of a Predecessor Rain Event (PRE) into OPNAVINST 3140.24F.

# LIST OF REFERENCES


Bosart, L. F., J.M. Cordeira, T.J. Galarneau, B.J. Moore, H.M. Archamault, 2012: An analysis of Multiple Predecessor Rain Events Ahead of Tropical Cyclones Ike and Lowell: 10–15 September 2008. *Mon. Wea. Rev.*, doi:10.1175/MWR-D-11-00163.1, in press. [Available online at http://journals.ametsoc.org/doi/abs/10.1175/MWR-D-11-00163.1]

Cote, M. R., 2007: Predecessor rain events in advance of tropical cyclones. M.S. thesis, Department of Atmospheric and Environmental Sciences, University at Albany, State University of New York, 200 pp. [Available online at http://cstar.cestm.albany.edu/CAP_Projects/Project10/index.htm]

Galarneau, T.J., L.F. Bosart, and R.S. Schumacher, 2010: Predecessor Rain Events ahead of Tropical Cyclones. *Mon. Wea. Rev.*, **138**, 3272–3297.

Naval Research Laboratory, Monterey California, 2009: The Typhoon Havens Handbook for the Western Pacific and Indian Oceans. [Cited: 2012 http://163.251.239.142/resources/yoko/training/typhoon/0start.htm]

Schumacher, R.S., T.J. Galarneau, and L.F. Bosart, 2010: Distant Effects of a Recurving Tropical Cyclone on Rainfall in a Midlatitude Convective System: A High-Impact Predecessor Rain Event. *Mon. Wea. Rev*., **139**, 650–667.

Commander, Fleet Activities Sasebo, 2010: CFASINST 3006.1B. Hazardous/Destructive Weather Plan.

Commander, Naval Maritime Forecast Center, Pearl Harbor HI, 2011: Naval Message: Prognostic Reasoning For Tropical Storm Roke 18W (Roke) Warning No. 21. Message DTG: 1500 (UTC) 16 Sep 2011.

Commander, United States Forces Japan, 2010: COMNAVFORJAPANINST 3140.4A. Hazardous/Destructive Weather Plan.

Harr, P.A. and Elsberry, R. L., 2000: Extratropical Transition of Tropical Cyclones over the Western Pacific. Part I: Evolution of Structural Characteristics during the Transition Process. *Mon. Wea. Rev.*, **128**, 2613–2663.

Martin, J.E., 2006: *Mid-Latitude Atmospheric Dynamics, A First Course.* John Wiley & Sons, 324 pp.

United States Department of the Navy, 2008: OPNAV INSTRUCTION 3140.24F. Adverse and Severe Weather Warnings and Conditions of Readiness. [Available online at http://doni.daps.dla.mil/OPNAV.aspx]

United States Department of the Air Forcem 2011: AIR FORCE INSTRUCTION 10-206. Operational Reporting. [Available online at http://www.af.mil/shared/media/epubs/AFI10-206.pdf]

Wallace, K. A., 2008: A Probabilistic Approach to Tropical Cyclone Conditions of Readiness (TCCOR). M.S. thesis, Dept. of Meteorology and Physical Oceanography, The Naval Postgraduate School, Monterey California, 65 pp. [Available online at http://www.dtic.mil/cgi-bin/GetTRDoc?AD=ADA488744]

# INITIAL DISTRIBUTION LIST

1. Defense Technical Information Center
   Ft. Belvoir, Virginia

2. Dudley Knox Library
   Naval Postgraduate School
   Monterey, California

3. Commander, Naval Meteorology and Oceanography Command
   John C. Stennis Space Center, MS

4. Commander, Joint Typhoon Warning Center
   Pearl Harbor, HI

5. Commander, Naval Oceanography Antisubmarine Warfare Center
   Yokosuka, Japan

6. Staff Weather Officer, 5th Air Force
   Yokota, Japan

7. Commander, 35th Operations Support Squadron / Weather Flight
   Misawa Air Base, Japan